Plant Physiology Preview. Published on March 30, 2017, as DOI:10.1104/pp.16.01282

EXO70C2 is a key regulatory factor for optimal tip growth of pollen

Lukáš Synek[1], Nemanja Vukašinović[1], Ivan Kulich[2], Michal Hála[1,2], Klára Aldorfová[1,2], Matyáš Fendrych[1], Viktor Žárský[1,2]

[1] Institute of Experimental Botany, v.v.i., The Czech Academy of Sciences, Rozvojova 263, 16502 Prague 6, Czech Republic

[2] Department of Experimental Botany, Faculty of Science, Charles University, Vinicna 5, 12844 Prague 2, Czech Republic

Present addresses:

L.S. – Center for Desert Agriculture, KAUST, Thuwal 23955-6900, Saudi Arabia

M.F. – Institute of Science and Technology, Am Campus 1, A-3400 Klosterneuburg, Austria

Author contributions:

L.S. designed and performed experiments, wrote the article; N.V. performed ami-RNA experiments and the pollen tube localization; I.K. studied the pollen tube cell wall composition and dynamics, writing; M.H. conducted yeast two-hybrid assays, K.A. performed pollen tube staining; M.F. cloned EXO70C1 and EXO70C2; V.Z. supervised the project and complemented the writing.

Funding information:

This work was supported by the Czech Science Foundation (grant no. 15-24711S). Part of the V.Z. and I.K. income is covered by the Ministry of Education of the Czech Republic (project no. NPUI LO1417).

One sentence summary:

EXO70C2, from the family of exocyst subunits, is a novel factor regulating pollen tube tip growth in Arabidopsis, and its paralog EXO70C1 has a partially redundant function.

Corresponding author email:

lukas.synek@kaust.edu.sa

Abstract

The exocyst, an eukaryotic tethering complex, co-regulates targeted exocytosis as an effector of small GTPases in polarized cell growth. In land plants, several exocyst subunits are encoded by double or triple paralogs, culminating in tens of EXO70 paralogs. Out of 23 Arabidopsis EXO70 isoforms, we analyzed seven isoforms expressed in pollen. Genetic and microscopic analyses of single mutants in *EXO70A2*, *C1*, *C2*, *F1*, *H3*, *H5*, and *H6* genes revealed that only a loss-of-function *EXO70C2* allele resulted in a significant male-specific transmission defect (segregation 40%:51%:9%) due to aberrant pollen tube growth. Mutant pollen tubes grown *in vitro* exhibited enhanced growth rate and a decreased thickness of the tip cell wall, causing tip bursts. However, *exo70C2* pollen tubes could frequently recover and restart their speedy elongation, resulting in a repetitive stop-and-go growth dynamics. A pollen-specific depletion of the closest paralog, *EXO70C1*, using ami-RNA in the *exo70C2* mutant background resulted in a complete pollen-specific transmission defect, suggesting redundant functions of EXO70C1 and EXO70C2. Both EXO70C1 and EXO70C2, GFP-tagged and expressed under their native promoters, localized in the cytoplasm of pollen grains, pollen tubes, and also root trichoblast cells. Expression of EXO70C2-GFP complemented aberrant growth of *exo70C2* pollen tubes. The absent EXO70C2 interactions with core exocyst subunits in the yeast two-hybrid assay, cytoplasmic localization, and genetic effect suggest an unconventional EXO70 function possibly as a regulator of exocytosis outside the exocyst complex. In conclusion, EXO70C2 is a novel factor contributing to the regulation of optimal tip growth of Arabidopsis pollen tubes.

Introduction

Pollen tubes transporting sperm cells elongate via tip growth within the intercellular space of the transmitting tract in pistils to double fertilize ovules. Pollen tubes growing exclusively at their tips can achieve a rapid growth rate that is dependent on polarized exocytosis (McKenna et al., 2009; Chebli et al., 2013). Once the polarity of a nascent germinating pollen tube is established, the endomembrane secretory machinery supported by the actin cytoskeleton and tip-focused calcium gradient delivers cell wall and plasma membrane (PM) materials along with cell wall-modification enzymes to the growing apex (reviewed in Cole and Fowler, 2006; Cheung and Wu, 2008; Hepler et al., 2013; Fu, 2015). Any perturbation in tip growth reduces the chance of an affected pollen tube to fertilize an ovule under competition with more fit ones (MacAlister et al., 2016).

At the pollen tube apex, we recognize the “clear zone” characterized by a network of highly dynamic short F-actin filaments and intensive trafficking of both exocytic and endocytic vesicles that form the inverted cone (reviewed in Hepler and Winship, 2015). The exocytic domain is located at the very tip or close to it (Sanati Nezhad et al., 2014; Bloch et al., 2016), then is followed with some partial overlap by the endocytic domain, which helps to remove the excess of membrane added by intensive exocytosis (Zonia and Munnik, 2008; Moscatelli and Idilli, 2009; Zonia and Munnik, 2009). Therefore, the balance between polarized exocytosis and endocytic recycling is a critical factor for proper tip growth. In growing pollen tubes, the cell wall composition changes in a gradient from mostly pectinaceous wall at the apex, followed by a cellulose layer generated later, and finally callose (Chebli et al., 2012).

Cell wall components or PM enzymes for their production are delivered to the cell surface in secretory vesicles (reviewed in Bashline et al., 2014). Tethering and docking of secretory vesicles to the PM at sites of intensive secretion is mediated by the exocyst, a tethering complex present in most eukaryotic lineages (reviewed in Heider and Munson, 2012; Vukašinović and Žárský, 2016), that is regulated by Rab and Rho small GTPases to achieve effective and spatially regulated exocytosis (reviewed in Wu et al., 2008; Žárský et al., 2010; Pfeffer, 2013). Therefore, the exocyst generally accumulates at PM domains characterized by intensive secretion, e.g. the growing bud in yeast (TerBush and Novick, 1995), tips of growing neurites (Vega and Hsu, 2001), lateral membranes of root epidermal cells (Fendrych et al., 2013; Zhang et al., 2016), or pollen tubes tips (Hála et al., 2008; Bloch et al., 2016). In plants, the exocyst has been implicated in cell elongation (Synek et al., 2006; Hála et al., 2008; Cole et al., 2014), xylem development (Li et al., 2013; Tu et al., 2015; Vukašinović et al., 2016), pollen-stigma interactions (Samuel et al., 2009; Kitashiba et al., 2011; Safavian et al., 2015), pectin deposition in seed coat development (Kulich et al., 2010), cell wall maturation in trichomes (Kulich et al., 2015), cytokinesis (Fendrych et al., 2010; Rybak et al., 2014), endosomal recycling (Drdová et al., 2013), and response to pathogens (Pečenková et al., 2011; Stegmann et al., 2012).

Structurally, the exocyst is an octameric complex composed stoichiometrically of Sec3, Sec5, Sec6, Sec8, Sec10, Sec15, Exo70, and Exo84 subunits that was originally discovered in budding yeast (TerBush et al., 1996, Guo et al., 1999). Plants encode all exocyst subunits (Cvrčková et al., 2001; Eliáš et al., 2003) that act together as a functional complex (Hála et al., 2008; Fendrych et al., 2010). Although exocyst subunits are typically encoded by one gene in Opisthokonts, they are often duplicated or even multiplicated in plants (Cvrčková et

al., 2001 and 2012; Vukašinović et al., 2014). The *EXO70* gene in particular has undergone a dramatic evolutionary expansion – e.g. 23 paralogs in *Arabidopsis thaliana*, or 47 in *Oryza sativa* (Synek et al., 2006; Cvrčková et al., 2012). Together with their differential expression (Synek et al., 2006; Li et al., 2010), this variety allows for a functional and tissue specialization, and is probably linked to the transition of plants from water to the challenging land conditions in the evolution (Žárský et al., 2013). The multiple EXO70s may act as exchangeable components of the exocyst complex that confer specific properties to the exocyst, and therefore each cell type might be endowed with a set of functionally distinct exocyst complexes directing different cargos to particular exocytic domains (Žárský et al., 2009 and 2013). Indeed, sub-functionalization of particular EXO70s implicated in autophagy-related transport to vacuoles (Kulich et al., 2013), light-induced stomatal opening (Hong et al., 2016), and plant periarbuscular membrane formation (Zhang et al., 2015) has been described.

In contrast, EXO70A1, a highly abundant isoform in the Arabidopsis sporophyte and a core exocyst subunit, plays a general "house-keeping" role in polarized exocytosis in multiple tissues, since its depletion cannot be fully compensated by other paralogs and has a dramatic effect on the entire plant growth and morphogenesis (Synek et al., 2006).

Although knock-out mutants in several exocyst subunits (SEC5a/b, SEC6, SEC8, and SEC15a) in Arabidopsis exhibit severe defects in pollen tube germination or growth, typically resulting in very short and depolarized pollen tubes and zero transmission of respective mutant alleles (Cole et al., 2005; Hála et al., 2008; Bloch et al., 2016), no EXO70 isoform analyzed so far displayed a comparable phenotype. Only a weak pollen-specific transmission defect was reported for an *exo70C1* mutant allele (Li et al., 2010). Recently, the PM localization of SEC3-GFP in Arabidopsis pollen tube tips was shown to predict the pollen tube growth direction (Bloch et al., 2016).

In this work, we aimed to identify EXO70 isoforms expressed in pollen and involved in pollen tube growth. We found that a single mutant in *EXO70C2* exhibits a significant male-specific transmission defect due to aberrant pollen tube growth characterized by inefficient cell wall deposition and increased rate of the pollen tube elongation, causing transient growth arrests and frequent partial or lethal pollen tube collapses. Further, we evidenced that EXO70C1, the closest paralog to EXO70C2, and to a minor extent also EXO70H3, play partially redundant roles. Surprisingly, our localization and interaction studies indicate that EXO70C2 and EXO70C1 may not act as stable subunits of the exocyst complex but rather acquired an unconventional function as regulators of tip growth.

137

138

139

Results

Several EXO70 isoforms, but not EXO70A1, are expressed in pollen

While several exocyst subunits are essential for pollen tube growth, the EXO70A1 subunit – essential in the sporophyte – is dispensable for pollen functions (Synek et al., 2006; Hála et al., 2008; Drdová et al., 2013). Indeed, EXO70A1 remained undetected in the pollen RNA-Seq and proteome analyses (Loraine et al., 2013; Grobei et al., 2009). These facts opened a question: which member(s) of the EXO70 family acquired the role of EXO70A1 in the pollen tube tip growth?

Microarray data (www.genevestigator.com – Zimmermann et al., 2004; bar.utoronto.ca/efp – Winter et al., 2007) fit recent RNA-Seq data on pollen transcriptome in Arabidopsis (Loraine et al., 2013) and provided hints that *EXO70C1*, *C2*, *H3*, and *H5* are highly abundant *EXO70* isoforms in pollen, while *EXO70A2*, *F1*, and *H6* are detected at lower levels in at least one stage of pollen development (Figure 1 A and B; Supplemental Figure 1). Interestingly, significant expression of *EXO70C1* and *EXO70C2* has been also detected in root trichoblast cells (Supplemental Figure 2). This dual (pollen-trichoblast) specificity points to their possible general involvement in the tip growth.

Given the multiple levels of mRNAs post-transcriptional regulations, we attribute a high importance to proteomic data that confirmed EXO70C1, C2, and A2in the mature Arabidopsis pollen, with EXO70C2 being the most abundant EXO70 isoform (Figure 1C) (Grobei et al., 2009; Mayank et al., 2012). EXO70C1 and EXO70C2 were identified also as phosphoproteins, pointing to new regulatory possibilities (Mayank et al., 2012). Surprisingly, EXO70H3 was not detected at the protein level despite its enormous transcript abundance, indicating a strong regulation of its expression at posttranscriptional or translational levels. All core exocyst subunits were also found in the mature pollen, with the numbers of peptides detected in remarkable agreement with the stoichiometry of the exocyst complex (Figure 1C).

Taken together, several EXO70 isoforms can play some role in the male gametophyte. Therefore, we started experimental analyses of reasonably supported candidates: EXO70A2 (At5g52340), EXO70C1 (At5g13150), EXO70C2 (At5g13990), EXO70F1 (At5g50380), EXO70H3 (At3g09530), EXO70H5 (At2g28640), and EXO70H6 (At1g07725).

The *EXO70C2* disruption results in a pollen-specific transmission defect

We obtained and characterized available T-DNA/transposon insertional mutants in *EXO70A2*, *C1*, *C2*, *F1*, *H3*, *H5*, and *H6* (Supplemental Figure 3). All homozygous mutant

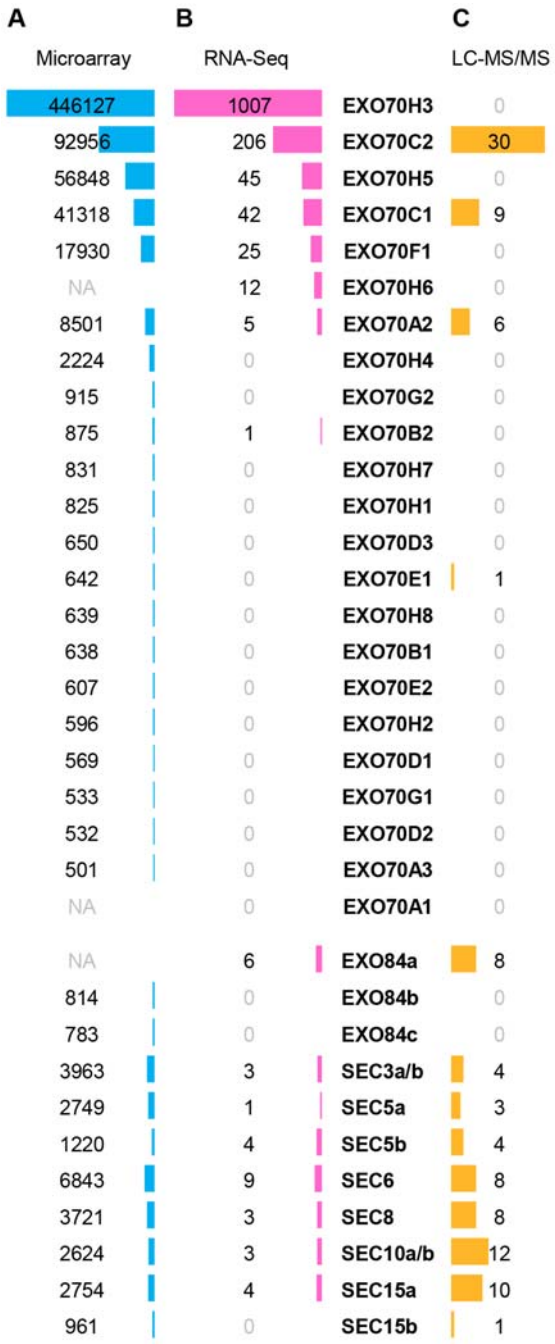

lines exhibited no obvious phenotypic changes in the sporophyte. Heterozygotes showed normal segregation ratio based on PCR genotyping, except for *exo70C2-1*, suggesting a significant transmission defect of this mutant allele (Table 1). Based on the segregation ratio 39.8% : 50.9% : 9.3%, we calculated the efficiency of the *exo70C2* pollen tubes in fertilization to be about 23% under the competition with WT pollen tubes (see an interactive model in Supplemental File 1). Reciprocal crosses followed by PCR genotyping of the offspring revealed that the *exo70C2-1* transmission defect is male-specific (Table 2).

In contrast to the two independent *exo70C1* knock-out lines (in the Col-0 background) with normal transmission analyzed here, the Ds-transposon allele CW841908 (i.e. CSHL_ET11742) in the Landsberg erecta background exhibited slightly reduced transmission efficiency (78%) via pollen (Li et al., 2010), albeit this insertion is located at a very similar position to the insertions above in the middle of the single *EXO70C1* exon. Furthermore, weak mutant alleles of *SEC8*, another exocyst subunit, showed normal transmission after self-crossing but significantly decreased after manual reciprocal crossing (Cole et al., 2005). For these two reasons, we performed reciprocal crossing of *exo70C1-1*, however only to confirm the normal *exo70C1-1* transmission in the Col-0 background (Table 2). The discrepancy between CSHL_ET11742 and *exo70C1-1* mutant alleles may be explained by specific behavior of EXO70C1 in different ecotypes.

Although the segregation ratio of *exo70H3* heterozygous mutants was not statistically different from normal segregation, the enormous abundance of *EXO70H3* transcripts in pollen led us to analyze *exo70H3 exo70C2-1* double mutants. The *exo70C2-1* transmission defect was more pronounced in the homozygous *exo70H3* background as documented by the 47.2% : 47.3% : 5.5% segregation ratio (Table 3), suggesting slightly redundant and or synergistic functions of EXO70C2 and EXO70H3. Additional comprehensive proteomic analyses will probably elucidate, why no hits were detected for EXO70H3 in the mature pollen (Grobei et al., 2009). Possibly, the abundant transcripts could be only translated after germination of pollen tubes or the protein is active at very low quantities.

In conclusion, EXO70C2 seems to play a prominent role among the candidate pollen EXO70s from the genetic point of view. Therefore, in our following work, we focused on the EXO70C2 isoform and its closely related paralog EXO70C1. (For next analyses we used exclusively *exo70C2-1* and *exo70C1-1* mutant lines; hereafter these alleles are designated *exo70C2* and *exo70C1*, respectively.)

The EXO70C1 activity is partially redundant with EXO70C2

As EXO70C2 is evolutionally very closely related to EXO70C1 (Synek et al., 2006; Cvrčková et al., 2012), we investigated whether these paralogs share redundant functions. Since crossing of *exo70C1* and *exo70C2* failed due to a strong genetic linkage of the two genes (the distance between At5g13150 and At5g13990 is 341 kbp, corresponding to approx. 2.2 cM), we attempted to inactivate both genes simultaneously using an artificial microRNA (amiRNA) against one gene in the knock-out mutant for the complementary gene.

We designed amiRNA (Schwab et al., 2006) targeted specifically against *EXO70C1* or *EXO70C2* and cloned them under the pollen-specific *LAT52* promoter. We introduced an amiRNA expression cassette against *EXO70C1* (hereafter as "amiRNAxC1") into *exo70C2* heterozygous mutants and an amiRNA expression cassette against *EXO70C2* (hereafter as "amiRNAxC2") into *exo70C1* heterozygous mutants using Agrobacterium-mediated transformation. T_1 plants resistant to Basta® (carried by the amiRNA cassette) and being WT or homozygous for the *exo70C1* or *exo70C2* mutant allele were used for subsequent analyses. The transmission efficiency of amiRNA cassettes was then determined as percentage of Basta® resistant seedlings in the T_2 population.

Our working hypothesis assumes that at least one of *EXO70C1* and *EXO70C2* genes must be active to allow for the amiRNA cassette transmission via pollen. T_1 transformants that are heterozygous for the amiRNA cassette will then provide differential segregation ratios in their offspring based on the combination of genotypes. For example, in the case of amiRNAxC2 in the *exo70C1* background, we can expect 50–75% of amiRNA-positive plants in the offspring, where 50% would indicate a complete pollen defect (amiRNA inherited only from the female), while 75% WT-like pollen.

Indeed, we recorded that amiRNAxC2 generated 44–56% of resistant seedlings in the *exo70C1* background, and amiRNAxC1 generated 49–52% of resistant seedlings in the homozygous *exo70C2* background (Table 4), suggesting minimal amiRNA transmission via pollen. An identical result was obtained when the presence of the amiRNAxC2 cassette was evaluated for one line by PCR genotyping on a parallel population, justifying the simple chemical selection approach (Table 4). The transmission of amiRNAxC1 or amiRNAxC2 in the WT background resembled the transmission of the *exo70C1* or *exo70C2* mutant allele, respectively, excluding thus that either amiRNA construct blocks the pollen function by itself (Table 4).

Furthermore, we performed reciprocal crossings of homozygous *exo70C1* mutants bearing amiRNAxC2 (heterozygous) with *exo70C1* homozygous plants without amiRNA, and evaluated the amiRNA cassette transmission by PCR genotyping of harvested crosses (Table 5). As a result, amiRNAxC2 could be transmitted only via the female gametophyte, indicating that the defects described above were pollen specific.

We conclude that the function of EXO70C1 is redundant to EXO70C2, because inactivation on both genes simultaneously led to a complete pollen-specific transmission defect in contrast to the partial defect in the case of the *exo70C2* single mutant.

Pollen tube growth is impaired in the *exo70C2* mutant

In order to address the cause of the pollen-specific transmission defect of the *exo70C2* allele, we examined pollen germination efficiency and pollen tube growth *in vitro* after 14h germination for homozygous and heterozygous *exo70C2* mutants and their WT siblings. Maximal pollen germination efficiency was comparable among all three genotypes (+/+: 91.7%, +/-: 88.3%, -/-: 90.1%; pollen of 20 plants for each genotype evaluated; >150 pollen grains per plant counted). However, pollen grains from homozygous mutants produced mostly shorter pollen tubes than WT with variable morphology (Figure 2).

The mutant and WT identity of short and long pollen tubes, respectively, was confirmed by crossing of *exo70C2* to the *quartet-1* background, where tetrads of sister pollen grains do not separate (Johnson-Brousseau and McCormick, 2004; Preuss et al., 1994). Indeed, two long and two short pollen tubes typically emerged from each tetrad of pollen from *exo70C2* heterozygotes germinated *in vitro* (Figure 3 A–D).

While initial polarity establishment of mutant pollen tubes was unaffected, they regularly exhibited branching and sharp bending after germination *in vitro* (Figure 3 G–I). Furthermore, their tips were sensitive to bursting (especially during microscopic manipulation), frequently causing effusions of cytoplasm and collapses (Figure 3 G–K). Occasionally they produced protoplast-like structures emerging from the apex (Figure 3 J–K) with indistinct propidium-iodide labeling around these structures (Supplemental Figure 4). The morphology of *exo70C2* pollen tubes is different from the pollen tube phenotype of mutants in core exocyst subunits (*sec5a/b*, *sec6*, *sec8*, and *sec15a*) that generate short, wide, and intact pollen tubes (Cole et al., 2005; Hála et al., 2008).

In contrast, *exo70C2* pollen tubes grown *in vivo* were much longer than those *in vitro*, often reaching basal ovules (Figure 3 L). This discrepancy may be explained by mechanical support of the transmitting tract, compensating the mutant pollen tube sensitivity (see further).

Mutant *exo70C2* pollen tubes display higher growth rate and insufficient cell wall deposition resulting in repetitive transient stops and bursts of the growing tip

The cytoplasm effusions and bursts of *exo70C2* pollen tubes tips led us to inspect cell wall morphology and growth dynamics. While WT pollen tubes displayed steady growth, accompanied by known regular low-amplitude oscillations, *exo70C2* pollen tubes grew with extreme fluctuations in their growth rate in a stop-and-go manner (Figure 4 A). Importantly, the growth rate measurement in 90-s intervals during a growing phase revealed that the averaged maximal growth rate in a population of *exo70C2* pollen tubes was 126% of the WT

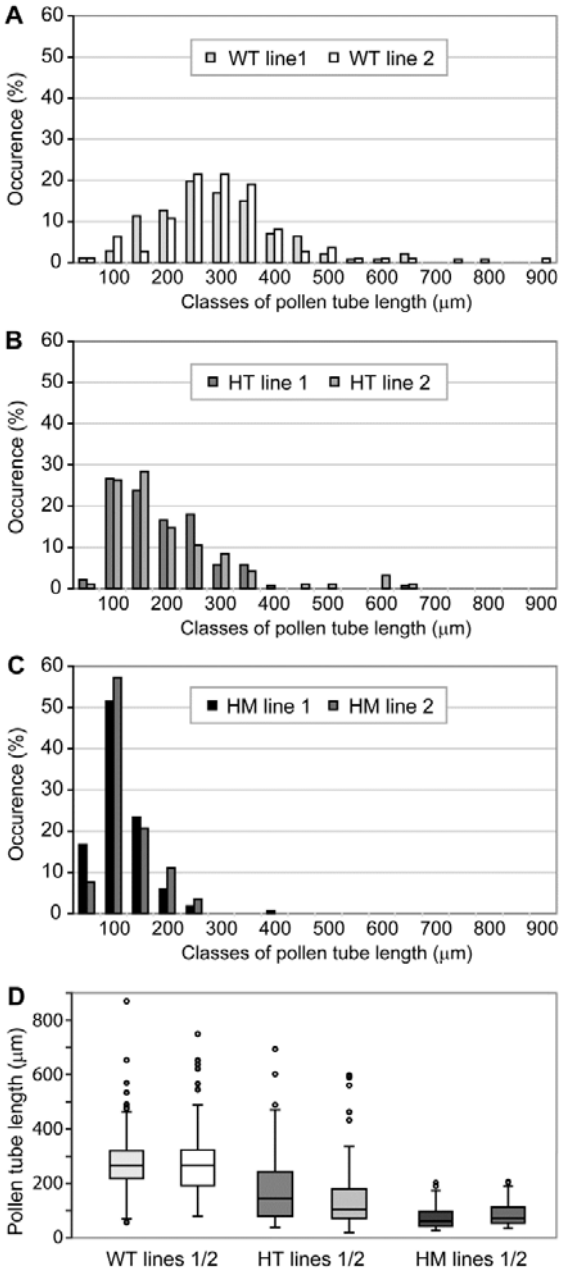

average (Figure 4 B). Detailed inspection of individual pollen tubes in 5-s intervals showed that *exo70C2* pollen tubes reached in peaks as much as 180% of the maximal WT growth rate (Figure 4 A). At the end of the high-speed growth period, the mutant pollen tubes burst, visibly extruding the cytoplasm (Supplemental Movie 1). This was most likely due to an insufficient cell wall formation, since the growth rate was inversely correlated with the cellulose and pectin deposition, as visualized by calcofluor white staining (Figure 4 A and C). When an *exo70C2* pollen tube elongated rapidly for a longer period, the apical calcofluor signal decreased even by 75% with respect to the WT control (Supplemental Movie 2).

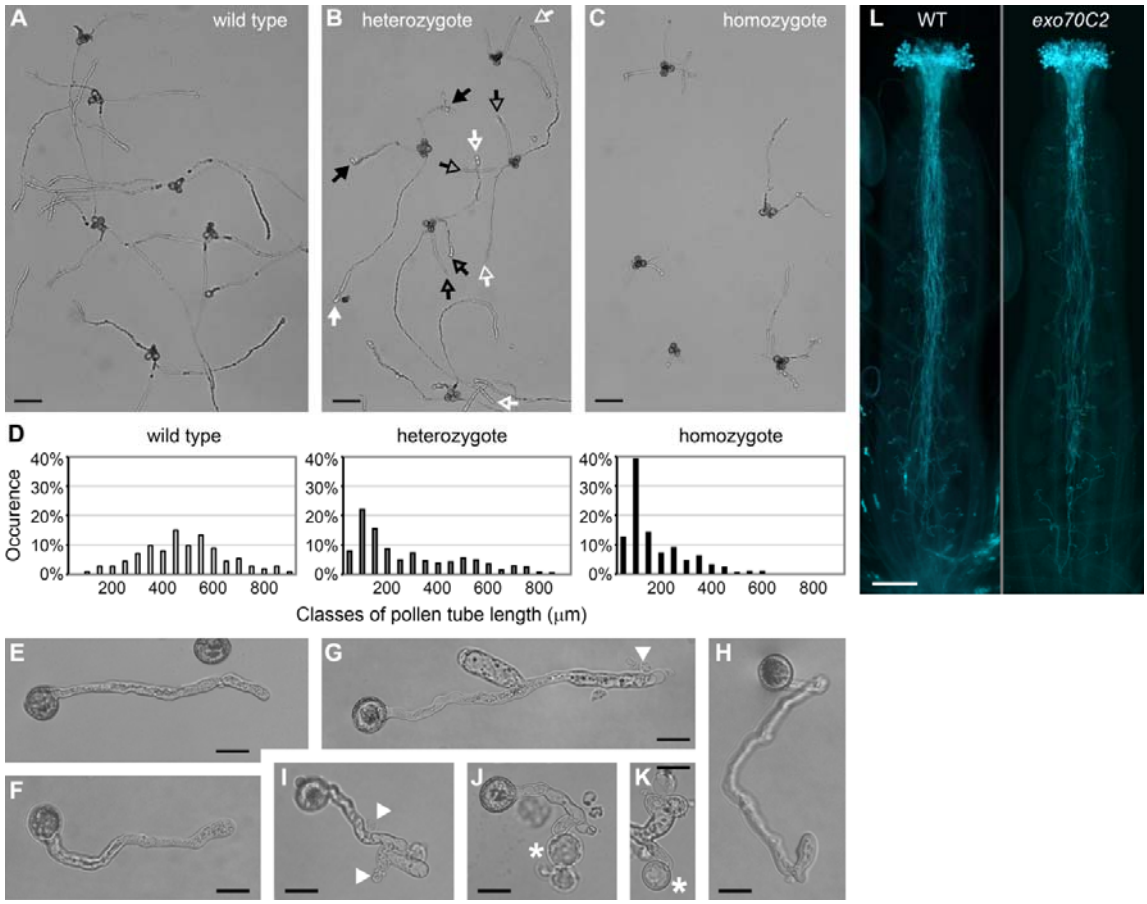

Furthermore, the insufficiency of cell wall materials at the cell surface corresponded to its retention in the cytoplasm, as visualized by ruthenium red, commonly used for staining of methylesterified pectins (Hou et al., 1999). Ruthenium red staining of pollen tubes in hypotonic conditions, causing extrusions of the cytoplasmic content, showed significantly stronger cytoplasmic pectin staining in *exo70C2* pollen tubes (Figure 4 D and E). However, live staining of external pectins in the cell wall using propidium iodide (proposed to bind demethoxylated homogalacturonan component of pectin; Rounds et al., 2011) was comparable to WT, except for more frequent patches of thicker pectin deposition, corresponding to events when a pollen tube stopped its growth or collapsed (Figure 4 F).

Surprisingly, the *exo70C2* pollen tubes grown *in vitro* could frequently recover after their burst and with certain delay restart their tip growth at the same apex or a new apex established in some distance back to the old one. We have observed multiple cycles of burst-recovery, however ultimately terminated with growth arrest or total collapse of the handicapped mutant pollen tube (Supplemental Movie 3).

We conclude that *exo70C2* mutant pollen tubes exhibit a significantly enhanced growth rate and compromised cell wall deposition at the growing apex as compared to WT, causing

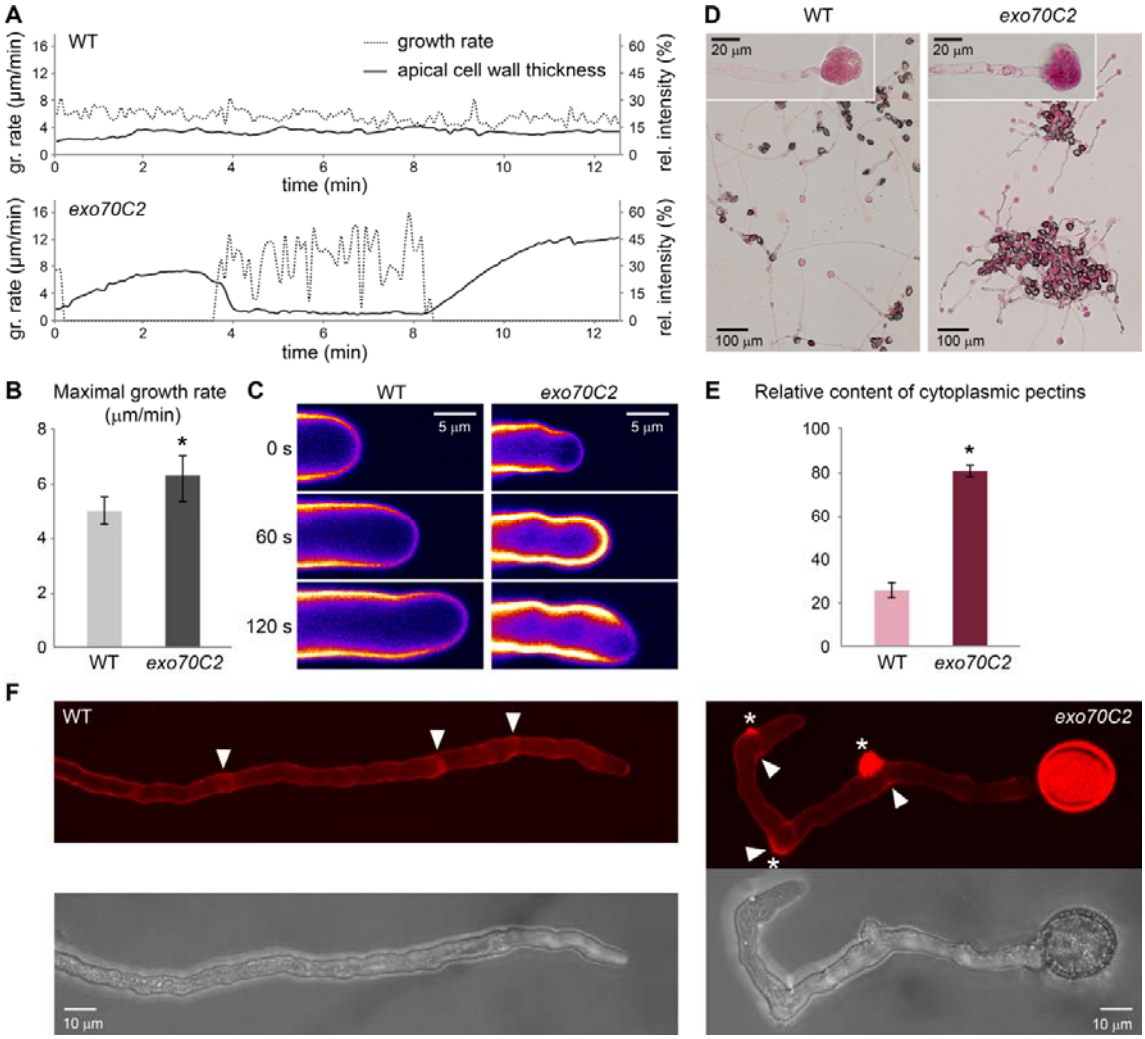

306 subsequently repetitive bursts of growing tips. This behavior explains why *exo70C2* pollen
307 tubes obtain the branched morphology and are ultimately significantly shorter than WT
308 siblings in suspension *in vitro* cultures.
309
310 **EXO70C2:GFP complements the *exo70C2* mutation**
311 To prove that the defects observed in pollen tubes are caused by dysfunction of the *EXO70C2*
312 gene, we tested *exo70C2* mutants for complementation with *EXO70C2:GFP* expressed under
313 the native *pEXO70C2* promoter (for localization of this fusion protein see the next chapter).
314 After selection of fluorescent plants heterozygous for the *exo70C2* allele and
315 homozygous for the *pEXO70C2::EXO70C2:GFP* expression cassette, we conducted
316 segregation analysis of the mutant allele in the offspring. As a result, the segregation ratio of
317 the *exo70C2* allele was statistically indistinguishable from the Mendelian ratio (+/+: 27.1%,
318 +/-: 49.2%, -/-: 23.7%; n = 118; χ^2 = 0.305, *P* value = 0.859), indicating that

pEXO70C2::EXO70C2:GFP can complement the *exo70C2* transmission defect. It also demonstrates the functionality of the EXO70C2:GFP fusion protein.

Furthermore, we used plants homozygous for the *exo70C2* allele and heterozygous for the *pEXO70C2::EXO70C2:GFP* expression cassette to characterize pollen tube growth of their pollen germinated *in vitro*. We measured pollen tube lengths of fluorescent and non-fluorescent pollen tubes separately within each sample (Figure 5 A). In agreement with the previous observation, the distribution of fluorescent pollen tubes lengths resembled WT characteristics, while the distribution of non-fluorescent pollen tubes lengths was similar to *exo70C2* mutant pollen tubes (Figure 5 B; compare to Figure 2 A and C). In addition, we used plants homozygous for both the *exo70C2* allele and the *pEXO70C2::EXO70C2:GFP* cassette, where all pollen tubes displayed fluorescence. In this combination, the distribution of fluorescent pollen tubes lengths resembled WT characteristics as expected (Supplemental Figure 5; compare to Figure 2A).

In conclusion, the *pEXO70C2::EXO70C2:GFP* expression complemented the *exo70C2* disruption in pollen tube growth.

EXO70C2 as well as EXO70C1 are localized in the cytoplasm of pollen tubes and trichoblast cells

In order to characterize tissue/cell specificity and subcellular localization of EXO70C2 and EXO70C1, we cloned each gene including its native promoter and fused it to *GFP* at its C-terminus. Localization of EXO70C2:GFP or EXO70C1:GFP was analyzed microscopically in their respective homozygous mutant backgrounds.

Both *pEXO70C2::EXO70C2:GFP* and *pEXO70C1::EXO70C1:GFP* were found specifically expressed in mature pollen grains, pollen tubes and trichoblast cells in roots (Figure 6), which is in agreement with available microarray data that do not indicate their expression in any other cell type/tissue (Genevestigator; Arabidopsis eFP Browser). Expression patterns of EXO70C2:GFP and EXO70C1:GFP were similar with a notable difference: The EXO70C1:GFP expression in roots started already in trichoblast precursors in the late meristematic zone, while the EXO70C2:GFP expression was first detectable in the elongation zone (Figure 6 C and H).

Both EXO70C2:GFP and EXO70C1:GFP localized to the cytoplasm without association with any distinct structures (Figure 6 B, F, G, H). In contrast to EXO70C2:GFP, EXO70C1:GFP exhibited a capacity to enter the nucleus – transiently after cytokinesis in trichoblast precursors in the root meristem (Figure 6 H) or permanently in developed

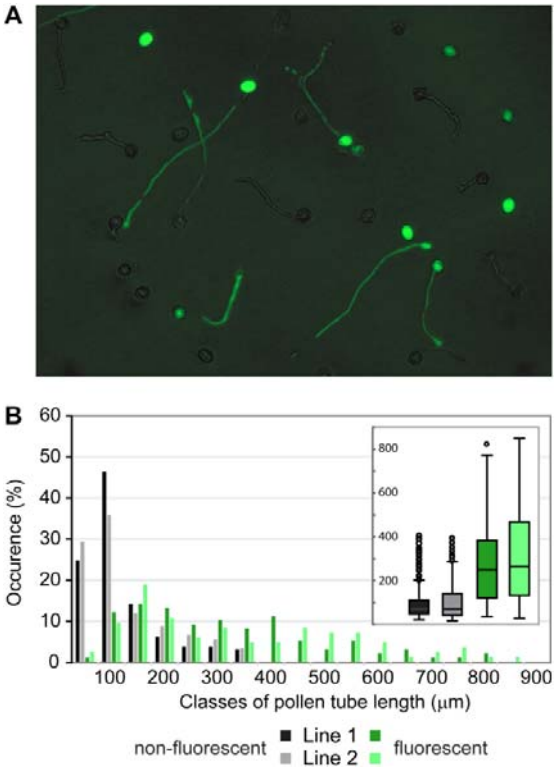

trichoblast cells and pollen grains (Figure 6 A and F), pointing to a potential nuclear regulatory function. Surprisingly, no PM signal was detectable for EXO70C1:GFP or EXO70C2:GFP, albeit all core exocyst subunits typically decorate the PM in various cell types with varying minor fraction in the cytoplasm (Fendrych et al., 2010 and 2013; Drdová et al., 2013; Zhang et al., 2016; Bloch et al., 2016).

To evaluate a possible impact of the GFP position on the subcellular localization of EXO70C2 an N-terminal GFP fusion (*pEXO70C2::GFP:EXO70C2*) was generated, and showed identical localization pattern to EXO70C2:GFP, excluding a negative effect of the GFP position (Supplemental Figure 6).

EXO70C2 does not co-localize or interact with core exocyst subunits

The undetectable EXO70C2 PM localization, unexpected for a putative exocyst subunit, led us to perform three comparative experiments to core exocyst subunits.

First, we localized two exocyst subunits, *pSEC8::*GFP:SEC8 and *pSEC10a::*SEC10a:GFP (Fendrych et al., 2010; Vukašinović et al., 2014), which are active in pollen and were cloned with their native promoters, in comparison to *pEXO70C2::*EXO70C2:GFP in growing Arabidopsis pollen tubes using a spinning disc confocal microscope under identical settings for all three fusion proteins. The imaging was performed in time series to prove that analyzed pollen tubes are growing normally and to

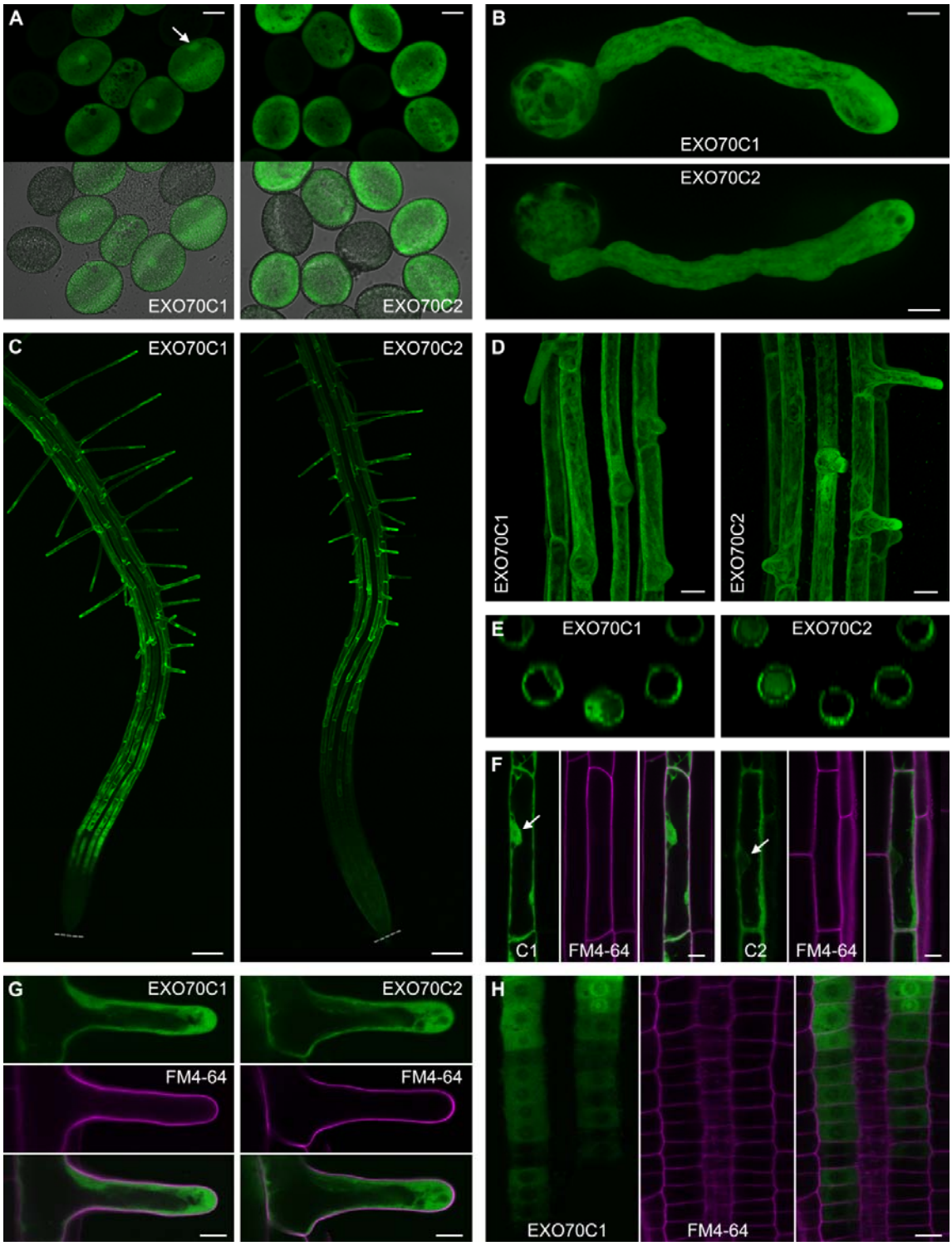

document possible localization dynamics. GFP:SEC8 and SEC10a:GFP showed an enrichment in the inverted cone and, importantly, accumulation in distinct patches along the PM at the pollen tube apex, in contrast to the cytoplasmic distribution of *pEXO70C2::*EXO70C2:GFP in the inverted cone and pollen tube shank without any decoration of the PM (Figure 7 A).

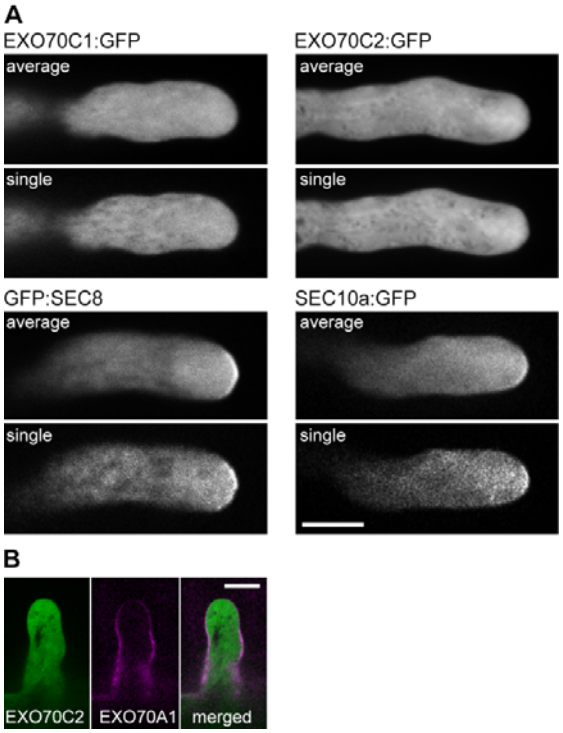

Second, we performed a direct comparison to another EXO70 isoform – EXO70A1, which is a sporophytic experimentally-proven exocyst subunit with described PM localization (Drdová et al., 2013; Fendrych et al., 2013; Zhang et al., 2016). Imaging in root hairs showed a PM decoration of developing root hairs by *pUBQ10::*RFP:EXO70A1, while *pEXO70C2::*EXO70C2:GFP was again found only in the cytoplasm in the same cell (Figure 7 B).

Third, since EXO70A1 interacts with SEC3a and the N-terminal half of EXO84b (EXO84b-N) in the yeast two-hybrid system (Hála et al., 2008; Fendrych et al., 2010), we tested EXO70C2 and also EXO70A2, another isoform highly abundant in the pollen proteome, for pair-wise interactions with exocyst subunits. While EXO70A2 did interact with SEC3a and EXO84b-N, and additionally with SEC10b, EXO70C2 showed no positive interactions neither as bait nor as prey (Figure 8 A). However, we found EXO70C2 interacting with ROH1 in the yeast two-hybrid system, a putative negative regulator of secretion, similar to the EXO70C1-ROH1 interaction published earlier (Kulich et al., 2010) (Figure 8 B).

Taken together, in spite of clear indications that EXO70C2 is involved in tip growth of pollen tubes, these observations favor a hypothesis that it probably does not serve as a stable functional subunit of the exocyst complex. On the other hand, EXO70A2 is likely incorporated to the exocyst complex as indicated by physical interactions with three core exocyst subunits.

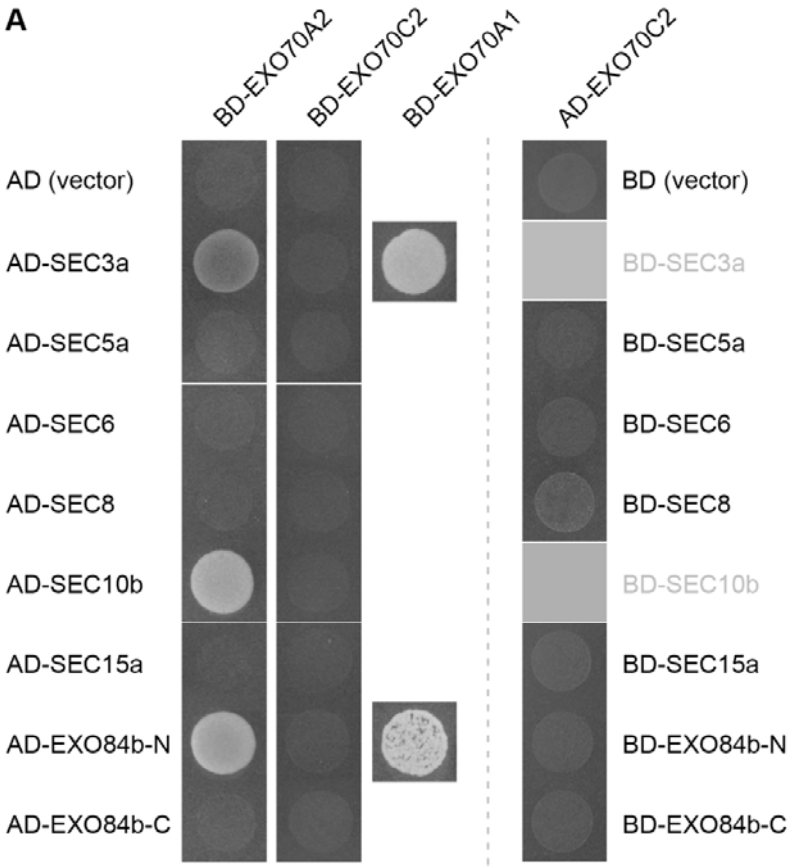

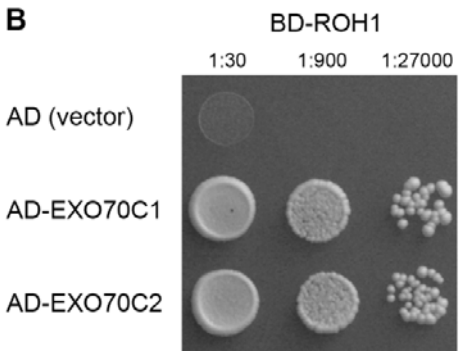

397

398

399

Discussion

EXO70C2 is a key factor for efficient pollen tube growth

Very limited experimental data on the EXO70 family in pollen provoked our interest to explore what EXO70 isoforms are expressed in pollen and engaged in tip growth of pollen tubes in Arabidopsis. We anticipated that another EXO70 isoform(s) adopted the essential role of sporophytic EXO70A1 in the male gametophyte. Our list of potential pollen EXO70 isoforms (EXO70A2, C1, C2, F1, H3, H5, and H6) is consistent, except for EXO70A2, with a comprehensive study on expression of all EXO70 family members in various tissues based on semi-quantitative RT-PCR and promoter activity by Li et al. (2010). The *EXO70C2* expression in later stages of pollen development was also proved by real-time PCR and RNA *in situ* hybridization (Lai, 2016).

Since only the *exo70C2* mutant allele showed a significant pollen-specific transmission defect resulting from pollen tube growth phenotypes, we propose that EXO70C2 is a key factor for efficient pollen tube growth. As the pollen transmission defect is not absolute, an additional EXO70 isoform(s) with redundant or synergistic functions must be responsible for the limited pollen tube growth in *exo70C2* mutants. Closely related EXO70C1 provides most likely such a function, because the simultaneous disruption of both EXO70C1 and EXO70C2 lead to non-functional pollen. EXO70C1 and EXO70C2 are the closest paralogs sharing 38% sequence identity at the protein level (which varies 14%–72% within the EXO70 family). On the other hand, the activity of EXO70C1 is not sufficient to compensate for the EXO70C2 loss of function, therefore we assume that its function is only partially redundant to EXO70C2 despite their identical spatio-temporal distributions in pollen. Alternatively, this insufficiency could be related to the lower EXO70C1 expression level. It remains to be investigated if EXO70C1 has some extra function or whether is serves only as a backup to EXO70C2. Limited contributing activity to the EXO70C1/2 function can be also attributed to EXO70H3.

Importantly, our analyses of the pollen-expressed EXO70 paralogs indicate, that the multiplicity of the EXO70 family in land plants could not be explained only based on the tissue/cell-specific expression as proposed by Li et al. (2010), but most probably several versions of the exocyst complex are active in land-plant cell types (Žárský et al., 2009, Žárský et al., 2013).

EXO70C2 involvement in the cell wall deposition

In comparison to WT pollen tubes, *exo70C2* pollen tubes exhibited significantly faster growth, which was interrupted by periods of growth arrest at very irregular frequency that were often a consequence of a pollen tube burst of various extend. Indeed, too high growth rate has been documented in loss-of-function mutants in NADPH oxidases to precede a pollen tube collapse (Lassig et al., 2014). The documented weakened cell wall at the tube apex during the rapid growth is most likely the primary cause of the *exo70C2* phenotype. Defects in cell wall deposition in seed coats, trichomes, cell plates, and xylem development have been well described for several Arabidopsis exocyst mutants (Fendrych et al., 2010; Kulich et al., 2010 and 2015; Li et al., 2013; Vukašinović et al., 2016). The delivery of methylesterified pectins, microfibrillar polysaccharides and fucosylated xyloglucans as possible exocyst cargo is most likely affected because they represent dominant components at the growing pollen tube tip (Chebli et al., 2012). Also mutants in hydroxyproline *O*-arabinosyltransferases (*HPAT1* and *HPAT3*), enzymes important for modifications of cell-wall extensins, exhibited a similar pollen tube phenotype to *exo70C2* (MacAlister et al., 2016). Whether the EXO70C2 (and EXO70C1) involvement in the regulation of secretion is direct or indirect remains to be elucidated, nevertheless we suggest below two major possible and opposing interpretations of the observed phenomenon.

First, since exocytosis of the plasma membrane material greatly exceeds the need for cell expansion in growing pollen tubes (Picton and Steer 1983), *exo70C2* could render a mild secretory defect, resulting in insufficient cell wall deposition, but still delivering enough membrane to support the rapid growth. This would lead into a rapid turgor-driven expansion, sensitive to bursts. The ratio of cellulose to other components of the cell wall would be possibly shifted. In agreement, an abnormal concentration of retained pectins in the cytoplasm was observed in the *exo70C2* pollen tubes. This interpretation could be also supported by the observation, that *in vivo* grown pollen tubes elongated more efficiently in comparison to *in vitro* conditions, probably due to stabilizing conditions in the transmitting tract, where the sensitive mutant pollen tubes tips are less vulnerable.

Another interpretation is that EXO70C2 acquired a negative regulatory function, negatively affecting cell expansion under normal circumstances by e.g. interfering with putative exocyst regulatory molecules such as small GTPases or lipids. EXO70C2 and EXO70C1 would then most probably contribute to the optimal balance between rates of vesicles delivery, exocytosis, and cellulose formation. This interpretation is in full agreement with previous experiments on NADPH oxidases in the tip growth. When two NADPH oxidases RBOHH and RBOHJ were knocked-out, the mutant pollen tubes exhibited higher

467 expansion rates than WT causing their burst (Lassig et al., 2014), similarly to the *exo70C2*
468 mutant. This implicates that NADPH oxidases negatively regulate pollen tube growth to
469 coordinate the rate of cell expansion with the rate of exocytosis. Such a regulation is a
470 plausible explanation also for the *exo70C2* mutant.
471
472 **Is EXO70C2 part of the exocyst complex?**
473 In spite of clear indications that EXO70C2 is involved in the regulation of secretion in pollen
474 tube tip growth and bearing in mind both hypotheses suggested above, we assume that
475 EXO70C2 (and EXO70C1) may not serve as a stable functional subunit of the exocyst
476 complex as it shows features distinct from conventional exocyst subunits, concerning the
477 morphology of mutant pollen tubes, PM localization, and physical interactions with exocyst
478 subunits. We reason that EXO70C1/C2 act as transient or indirect modulators of the exocyst,
479 resulting in optimal balance between the cell wall biogenesis and surface growth.
480 Outside of the exocyst complex, EXO70C1/C2 could very likely affect secretion via
481 ROH1, whose up-regulation results in decreased seed coat mucilage layer (Kulich et al.,
482 2010), and that is highly up-regulated in germinating pollen and root trichoblast cells
483 (Arabidopsis eFP Browser). ROH1 is a putative negative regulator of secretion, which is
484 known to bind EXO70C1 and EXO70A1 (Kulich et al., 2010), and here we report binding
485 toEXO70C2 as well. The absence of EXO70C2 and insufficient activity of EXO70C1 in the
486 *exo70C2* knock-out would lead to a release of an interfering or negative regulation of
487 exocytosis, and subsequently to the increased pollen tube growth rate, rendering the unstable
488 growth with stop-and-go dynamics accompanied by series of the tip burst and recovery, and
489 finally resulting in a pollen tube collapse. The identified EXO70C2 and EXO70C1
490 phosphorylation (Mayank et al., 2012) could also play a role in this regulation.
491 EXO70C1/C2 might also gain novel functions in the regulation of polarized exocytosis
492 unrelated to the exocyst. As postulated earlier (Žárský et al., 2013), it is highly probable that
493 the diversified plant EXO70 isoforms acquired specific functions (even unrelated to the
494 exocytosis), since in yeast and animal cells, the single EXO70 destabilizes tubulin
495 cytoskeleton (Wang et al., 2004), influences actin dynamics (Zuo et al., 2006; Liu and Guo
496 2012), lamellipodia formation by membrane deformation (Zhao et al., 2013), or pre-mRNA
497 splicing (Dellago et al., 2011). First examples of EXO70 sub-functionalization in Arabidopsis
498 and Medicago have been already published (see introduction).
499 If EXO70C2 and EXO70C1 are indeed not stable subunits of the exocyst complex,
500 EXO70A2 is then a good candidate for the core EXO70 subunit of the pollen exocyst as the

closest paralog to the prevalent sporophytic EXO70A1 exocyst subunit (72% sequence identity), and because its yeast two-hybrid interactions with other exocyst subunits were also similar to EXO70A1. Sekereš et al. (2017) documented the tobacco EXO70A paralog to be positively involved in exocytosis during tobacco pollen tube tip growth as a part of the exocyst complex.

EXO70C1 and EXO70C2 as common factors for tip growth in both male gametophyte and sporophyte

The localization pattern of GFP-tagged EXO70C1/C2 in Arabidopsis tissues fully matches the microarray data that indicate their pollen and trichoblast expression (Arabidopsis eFP Browser). Interestingly, this dual tissue specificity was suggested earlier based on a computational comparison of a translated Arabidopsis transcriptome with a soybean proteome (Cvrčková et al., 2010). Since root hairs produced by trichoblast cells and pollen tubes represent prime examples of tip growth in plants, it is likely that the EXO70C1/C2 regulatory module is specifically recruited to modulate this mode of cell expansion based on highly polarized tip-focused secretion. A number of regulators specific to polar growth is logically strongly correlated with EXO70C1/C2, including three RAB GTPases, ROP-GEF3/11/12, and transcription factors – all representing their potential interacting partners (ATTED-II; Genevestigator). Especially, a co-operation with ROP GTPases, major regulators of cell polarity, is highly probable, because their interaction with exocyst subunits EXO70B1 and SEC3 has been already documented (Hong et al., 2016; Lavy et al., 2007). Future experimental work will likely reveal additional functional interactions of EXO70C2 and EXO70C1 with other players involved in tip growth and elucidate the precise mechanism of their action.

Although well-curated transcriptomic data for pollen-specific gene expression in other Angiosperm species apart from Arabidopsis and rice are scarce (Rutley and Twell, 2015), a mere comparison of these two species indicates that the EXO70C class is most probably related to pollen tube development in all Angiosperms, suggesting conservation of the EXO70C expression across monocots and dicots (Add. File 8 in Wei et al., 2010). This notion is supported by the tight clustering and relatively low divergence of EXO70C representatives in the EXO70 phylogenetic tree (Cvrčková et al., 2012).

Conclusions

Pollen tubes characterized by their specific mode of elongation – the tip growth – represent an established model system for studies of cell expansion and its regulation in plant cell biology. Although the exact molecular mechanism of EXO70C1/C2 functions and the roles of other pollen EXO70 isoforms remain to be elucidated, we clearly demonstrated the importance of EXO70C1/C2 for optimal pollen tube growth via the exocytosis moderation, and thus revealed novel players in the complex network of the tip growth regulation.

Materials and Methods

Plant material

Mutant plants of *Arabidopsis thaliana* were obtained from NASC (SALK T-DNA lines in the Columbia-0 ecotype; Alonso et al., 2003), GABI-Kat (GABI T-DNA lines in the Columbia-0 ecotype; Kleinboelting et al., 2012) and Riken (RATM transposon lines in the Nossen-0 ecotype; Ito et al., 2002; Kuromori et al., 2004). Following lines were used in this study: *exo70A2* (GABI_824D06), *exo70C1-1* (GABI_100A02), *exo70C1-2* (GABI_334D05), *exo70C2-1* (RATM16-1469-1), *exo70C2-2* (SALK_045767), *exo70F1* (SALK_036927), *exo70H3* (GABI_651C10), *exo70H5* (SALK_007810), *exo70H6* (SALK_016535), and *qrt1-1* (CS8050; Preuss et al., 1994). Mutant plants were identified by selection when possible (GABI and RATM lines) and confirmed by PCR genotyping, then backcrossed to WT (Col-0).

Positions of insertions were verified by sequencing of PCR products obtained from ends of T-DNA/transposon insertions: *exo70A2* (-160 bp), *exo70C1-1* (+985 bp), *exo70C1-2* (+1030 bp), *exo70C2-1* (+788 bp), *exo70C2-2* (-405 bp), *exo70F1* (+179 bp), *exo70H3* (+31 bp), *exo70H5* (-63 bp), *exo70H6* (-28 bp) – positive or negative numbers refer to nucleotide positions downstream or upstream, respectively, of the start codon in the genomic sequence.

Genotype analysis and semi-quantitative RT-PCR

DNA from mutant plants was extracted from 20 mg of fresh leaves as described in Edwards et al. (1991). Plants were genotyped using PCR with T-DNA-specific (LBb1, o8760) or transposon-specific (Ds5-2a) primers and gene-specific primers – all listed in Supplemental Table 1.

To test for the presence of gene transcripts in mutant plants, total RNA was isolated from 100 mg of flowers using the RNeasy kit (Qiagen). cDNA was synthesized using the Transcriptor High Fidelity cDNA synthesis kit (Roche). Levels of transcript abundance were analyzed by semi-quantitative PCR with gene-specific pairs of primers (Supplemental Table 1). *ACTIN7* was amplified as a quantitative control. Lines *exo70C1-1*, *exo70C1-2*, *exo70C2-1*, *exo70F1*, *exo70H3*, *exo70H5, exo70H6* were shown to be knock-outs; *exo70C2-2* with a promoter insertion produced *EXO70C2* transcripts at wild-type level; *exo70A2* with a promoter insertion displayed overexpression of *EXO70A2* (Supplemental Figure 3).

Plant cultivation

Seeds were surface sterilized (70% ethanol for 3 min, 10% commercial bleach for 10 min, and rinsed three times in sterile distilled water) and stratified for 3 days at 4°C. Seeds were then germinated on vertical ½ MS1 agar plates (½× Murashige and Skoog medium [Duchefa Biochemie] supplemented with 1% sucrose, vitamin mixture and 1.6% Plant agar [Duchefa Biochemie]) at 21°C and 16 h of light per day. The Riken RATM16-1469-1 1ine, GABI lines, and *qrt1-1* mutants were selected (when segregation was out of the interest) on ½ MS1 agar plates with hygromycin (20 µg/ml), sulfadiazine (7.5 µg/ml), or Basta® (50 µg/ml), respectively. Eight-day-old seedlings were transferred into turf pellets (Jiffy Products International, Norway) and grown again at 22°C and 16 h of light per day.

Preparation of amiRNA-driven knock-down lines

Artificial microRNAs (amiRNA) against *EXO70C1* and *EXO70C2* (At5g13150, At5g13990) were designed using the on-line microRNA designer (http://wmd3.weigelworld.org/cgi-bin/webapp.cgi), then PCR amplified from the pRS300 vector as described by Schwab et al. (2006). Resulting amiRNA cassettes were cloned using *Xho*I and *Nco*I into pWEN240 under the *LAT52* promoter. Finally, amiRNA cassettes including the LAT52 promoter were further PCR-amplified and subcloned to the pBAR1 vector using *Xma*I and *Xba*I. Sequences and primers are listed in Supplemental Table 1.

Resulting constructs with amiRNAxC1 or amiRNAxC2 were transformed by Agrobacterium-mediated transformation (Clough and Bent, 1998) into heterozygous mutants in *EXO70C2* or *EXO70C1*, respectively. Primary transformants (T_1) were selected for Basta® (phosphinothricin) resistance, and the presence of amiRNA cassettes was verified by PCR genotyping. Transmission of amiRNA cassettes was further analyzed based on the Basta® resistance of T_2 seedlings. Primer sequences are listed in Supplemental Table 1.

602

603 ***In vitro* Arabidopsis pollen germination**

604 Pollen was germinated on microscopic slides in 40-µl droplets of fresh germination medium
605 (10% sucrose, 1.6 mM 0.01% H_3BO_3, 1 mM $CaCl_2$, 1 mM $MgSO_4$, 1 mM $Ca(NO_3)_2$, pH
606 adjusted to 7.5). Pollen grains from fully open flowers were spread onto each droplet and one
607 extracted pistil was dipped into each droplet. For confocal microscopy and kinetics,
608 germination medium solidified with 1% low-melting-point agarose (Duchefa) was applied in
609 a thin layer into a chambered coverglass Lab-Tek II (Thermo Scientific). Slides or chambers
610 were enclosed to a humid chamber and incubated in a plant growth room at 22°C for 4 h
611 (samples for pollen tube morphology and live staining) or 14 h (samples for pollen tube
612 length), if not indicated differently.

613

614 **Germination efficiency and pollen tube morphology**

615 Images of *in vitro* germinated pollen (14 h) were taken using Olympus BX-51 with an
616 UPlanFL N 10x/0.3 (long working distance objective), DIC optics, epifluorescence filter sets,
617 and a DP50 camera (Olympus). The field aperture was nearly closed to enhance the depth of
618 focus.

619 Pollen grains were supposed as germinated when pollen tube length reached at least one
620 half of pollen grain diameter. Pollen tube length was measured in the AnalySIS software
621 (Olympus). Details of pollen tube morphology in brightfield were taken using an UPlanFL
622 20x/0.5 or UPlanFL 40x/0.75 and DIC optics on Olympus BX-51.

623

624 **Callose staining in pistils**

625 Self-pollinated pistils were harvested approx. 12 h after opening of anthers. Callose staining
626 with aniline blue in the pistils was done according to Mori et al. (2006) and imaged using a
627 Nikon 90i microscope with a PlanApo 4x/0.2 objective and a Clara camera (Andor).

628

629 **Live staining of pollen tubes with fluorescent dyes**

630 Propidium iodide, calcofluor white, FM4-64 or aniline blue were diluted in liquid
631 germination medium and applied gently onto *in vitro* germinated pollen before imaging.
632 Images were captured using a Zeiss LSM 880 confocal laser scanning microscope with Plan-
633 Apochromat 10x/0.45, Plan-Apochromat 20x/0.8, C-Apochromat 40x/1.2 WI, and C-
634 Apochromat 63x/1.2 WI objectives. Working concentrations, excitations and the range of

recorded emission were as follows: propidium iodide – 30 μM, 514 nm/566–719 nm, calcofluor white – 1 μg/ml, 405 nm/400–500 nm.

Measurement of pollen tube growth kinetics

For evaluation of the maximal growth rate, pollen tubes were germinated on the solidified germination medium. Then, 4 positions with *exo70C2* pollen and 4 with WT pollen were imaged for 5 hours, each position every 90 s, using a Nikon 90i microscope with a PlanApo 10x/0.45 objective and a Clara camera (Andor) generating 1392 x 1040 px images. The growth rate was then calculated by measuring a difference in pollen tube length between frames using Fiji ImageJ (Schindelin et al., 2012). For the maximal pollen tube growth rate, values lower than 0.1 μm/min were excluded. The experiment was done in a triplicate with very similar results.

For the pollen tube kinetics, germinated pollen was stained with calcofluor white (1 μg/ml) diluted in liquid germination medium. Each pollen tube was continuously imaged every 5.3 s using a Zeiss LSM 880 confocal laser scanning microscope with C-Apochromat 40x/1.2 WI, excitation 405 nm, emission recorded at 400–500 nm. The growth rate was then determined as above and the calcofluor white signal was measured as a mean intensity in a region of 20x30 pixels at the pollen tube apex through images with 14 px/μm resolution (cut-outs 300x140 px are presented in Figure 4C).

Ruthenium red staining

Pollen tubes germinated on solid medium were covered 0.0001% ruthenium red solution in distilled water to induce pollen tube burst and stain cytoplasmic pectins. The WT and mutant pollen was always applied side by side on one glass slide. Images (1392 x 1040 px) were taken using a Nikon 90i microscope with a PlanApo 10x/0.45 or PlanApo 40x/0.95 objectives and a Clara camera (Andor). Staining intensity was quantified only in the extruded cytoplasm as relative intensity in the red channel after subtraction of the background.

Cloning of gene constructs with GFP and RFP

pEXO70C1::EXO70C1:GFP was prepared by PCR amplification of a promoter region 1507 bp upstream from the start codon together with the *EXO70C1* CDS (At5g13150) without stop codon from genomic DNA, bordered by *Sal*I and *Not*I restriction sites (primer sequences in Supplemental Table 1), and cloned into *Sal*I and *Not*I sites in pENTR3C Gateway vector (Invitrogen). This sequence was further transferred using LR clonase II (Invitrogen) to

669 pGWB4 Gateway vector (Nakagawa et al., 2007). The construct was then transformed by
670 Agrobacterium-mediated transformation (Clough and Bent, 1998) to *exo70C1-1* homozygous
671 mutants.
672 *pEXO70C2::EXO70C2:GFP* was generated analogically but with addition of *Bgl*II and
673 *Not*I restriction sites to the ends of the CDS (At5g13990) and cloning into *Bam*HI and *Not*I
674 sites in the pENTR3C vector (Invitrogen). The construct was then introduced to WT plants by
675 Agrobacterium-mediated transformation and after selection crossed to homozygous *exo70C2-*
676 *1* mutants (the pGWB4 vector and Tn-insertion share the same hygromycin resistance,
677 excluding a direct transformation of mutants). The presence of both the mutant allele and the
678 introduced expression cassette was checked by PCR genotyping (primer sequences in
679 Supplemental Table 1).
680 To prepare *pEXO70C2::GFP:EXO70C2*, the amplified *EXO70C2* CDS bordered by *Xba*I
681 sites was first cloned into pBAR1-GFP vector using the *Xba*I site. *GFP:EXO70C2* was then
682 re-amplified from pBAR1 with addition of attB2 sequence at the 3'-end, and fused in
683 subsequent overlapping PCR to the amplified promoter bordered by attB1 sequence at its 5'-
684 end and a fragment of *GFP* at its 3'-end. This product was then cloned into pDONR201
685 (Invitrogen) using BP clonase II (Invitrogen) and finally transferred to pGWB1 (Nakagawa et
686 al., 2007) using LR clonase II (Invitrogen). All primer sequences are listed in Supplemental
687 Table 1. The construct was transformed to heterozygous *exo70C2-1* mutants.
688 To prepare *pUBQ10::RFP:EXO70A1*, the PCR-amplified *EXO70A1* CDS (At5g03540)
689 was inserted into pENTR3C (Invitrogen) using *Eco*RI and *Not*I (primer sequences in
690 Supplemental Table 1) and subsequently transferred to pUBN-RFP using LR clonase II
691 (Invitrogen). The construct was introduced by Agrobacterium-mediated transformation into
692 *exo70A1-2* heterozygous mutants (Synek et al., 2006) and selected on Basta®.
693
694 **Imaging of GFP-tagged EXO70C2/EXO70C1 and exocyst subunits**
695 For complementation assays, EXO70C2:GFP was imaged using the Olympus BX-51 with an
696 eGFP-specific narrow-pass filter set and mixed with bright field. At least 120 pollen tubes
697 were then measured for each line in the AnalySIS software (Olympus).
698 Cellular localization of GFP-tagged EXO70C1/C2 was performed in chambered
699 coverglass Lab-Tek II (Thermo Scientific) using a Zeiss LSM 880 confocal laser scanning
700 microscope equipped with Plan-Apochromat 10x/0.45, Plan-Apochromat 20x/0.8, C-
701 Apochromat 40x/1.2 WI objectives. FM4-64 (5 μM) was applied before imaging to visualize

PM. After excitation with 488-nm laser, emitted fluorescence of GFP and FM4-64 was recorded at 493–535 nm and 575–650 nm, respectively.

Dynamic localization of EXO70C2, EXO70C1, SEC8, and SEC10a in pollen tube tips was performed using a spinning disc confocal microscope (Yokogawa CSU-X1 on Nikon Ti-E platform, Agilent MLC400 laser box, Zyla sCMOS camera (Andor), NIS Elements 4.1 software). Exposure time was 300 ms, 4x averaging, 488-nm laser power 75%, and the images were taken every 4 s using a PlanApo 100x/1.4 lens. Five neighboring imaged were aligned and averaged for final figures.

Yeast two-hybrid assay

To test interactions of EXO70C2 with exocyst subunits, we prepared two different fusions of EXO70C2 with DNA-binding domain (BD) or Activating domain (AD): the full-length *EXO70C2* CDS was PCR-amplified with the stop codon and bordered with *Nde*I and *Sma*I restriction sites, then digested and cloned into the pGBKT7 vector or pGADT7, respectively (Clontech). *EXO70A2* CDS (At5g52340) was cloned analogically using *Eco*RI and *Sal*I sites in pGBKT7. *SEC15a* CDS (At3g56640) was bordered with *Bam*HI and *Sal*I sites and cloned into *Bam*HI and *Xho*I in pGADT7. Primers for cloning are listed in Supplemental Table 1. Exocyst genes fused to *AD* or *BD* as well as *BD-ROH1* and *AD-EXO70C1* were cloned previously (Hala et al., 2008; Kulich et al., 2010).

The yeast two-hybrid screening employed the MATCHMAKER GAL4 Two-Hybrid System 3 (Clontech) following manufacturer's protocols. Yeast strain AH109 was stepwise transformed. Prior to the second step, expression of the fusion proteins was verified by Western blotting using a rabbit polyclonal anti-GAL4-BD or anti-GAL4-AD antibody (1: 1000, Sigma), respectively, according to the manufacturer's recommendations. Double transformed cells were selected on -Leu -Trp medium. Single colonies were then scale-diluted in sterile water and dropped by 10 µl onto -Ade -His -Leu -Trp selective medium.

Tables

Table 1. Segregation of heterozygous mutants in putative pollen *EXO70* isoforms.

Allele	+/+	+/-	-/-	n	χ^2 test	*P* value	Line

expected	25.0%	50.0%	25.0%				
exo70A2-OE	26.7%	51.7%	21.7%	120	0.733	0.693	GABI_824D06
*exo70C1-1**	24.0%	50.0%	26.0%	150	0.120	0.942	GABI_100A02
exo70C1-2	24.6%	49.1%	26.3%	118	0.102	0.950	GABI_334D05
*exo70C2-1**	39.8%	50.9%	9.3%	159	30.037	<0.001	RATM16-1469-1
*exo70C2-2***	24.5%	48.1%	27.4%	106	0.321	0.853	SALK_045767
exo70F1	21.9%	53.3%	24.8%	105	0.638	0.727	SALK_036927
exo70H3	23.0%	56.0%	21.0%	100	1.520	0.468	GABI_651C10.03
exo70H5	23.2%	48.2%	28.6%	112	0.786	0.675	SALK_007810
exo70H6	26.0%	44.8%	29.2%	154	1.987	0.370	SALK_016535

+/+ = WT plants; +/- = heterozygous mutants; -/- = homozygous mutants; OE – overexpressor line

* these alleles were used for next analyses

** T-DNA insertion in the promoter; transcripts present at WT level

Table 2. Reciprocal crossing of *exo70C2* and *exo70C1* mutants to the wild type (Col-0).

Allele	**Pollen donor: +/-** **Pollen recipient: +/+**					**Pollen donor: +/+** **Pollen recipient: +/-**				
	+/+	**+/-**	**χ^2 test**	***P* value**	**n***	**+/+**	**+/-**	**χ^2 test**	***P* value**	**n***
expected	50.0%	50.0%				50.0%	50.0%			
exo70C2-1	87.5%	12.5%	63.00	<0.001	112	49.1%	50.9%	0.035	0.851	114
exo70C1-1	49.1%	50.9%	0.034	0.853	116	51.8%	48.2%	0.145	0.703	110

+/+ = WT plants; +/- = heterozygous mutants

* seeds from at least six independent crosses

747 **Table 3.** Segregation of *exo70C2* heterozygotes in the homozygous *exo70H3* mutant
748 background.
749

Allele	+/+	+/-	-/-	**n**	**χ^2 test**	***P* value**
normal	25.0%	50.0%	25.0%			
exo70C2-1	39.8%	50.9%	9.3%			
exo70C2-1	47.2%	47.3%	5.5%	146	* 51.411	* <0.001
in exo70H3					** 4.713	** 0.095

750
751 +/+ = WT plants; +/- = heterozygous mutants
752 * Chi-square test related to the normal segregation
753 ** Chi-square test related to the *exo70C2-1* single mutant segregation
754
755
756 **Table 4.** Transmission of amiRNA cassettes targeting *EXO70C1* or *EXO70C2*.
757

Plant	**amiRNA**	**Background genotype**	**Plants bearing amiRNA cassette in the offspring**	**n**	**Comments**
	xC2	*exo70C1*	50%		expected for a functional construct
	xC2	*exo70C1*	75%		expected for a non-functional construct
#1	xC2	*exo70C1*	53%	128	PCR genotyping
#1	xC2	*exo70C1*	52%	195	Basta® selection
#2	xC2	*exo70C1*	44%	116	Basta® selection
#3	xC2	*exo70C1*	56%	81	Basta® selection
	xC2	WT	60%*		expected for a functional construct
	xC2	WT	75%		expected for a non-functional construct
#7	xC2	WT	63%	230	Basta® selection
#8	xC2	WT	65%	249	Basta® selection
	xC1	*exo70C2*	50%		expected for a

	xC1	*exo70C2*	75%		functional construct expected for a non-functional construct
#4	xC1	*exo70C2*	49%	174	Basta® selection
#5	xC1	*exo70C2*	52%	107	Basta® selection
#6	xC1	*exo70C2*	52%	109	Basta® selection
	xC1	WT	75%		expected for a functional construct
	xC1	WT	75%		expected for a non-functional construct
#9	xC1	WT	79%	100	Basta® selection
#10	xC1	WT	76%	382	Basta® selection

* estimated based on the transmission efficiency of the *exo70C2-1* allele

Table 5. Transmission of the amiRNA targeting *EXO70C2* in the *exo70C1* homozygous mutant background via male or female gametophyte.

Pollen donor: amiRNAxC2 in *exo70C1*				
Pollen recipient: *exo70C1*				
+	**-**	**χ^2**	***P* value**	**n**
0%	100%	142.00	<0.001	142

Pollen donor: *exo70C1*				
Pollen recipient: amiRNAxC2 in *exo70C1*				
+	**-**	**χ^2**	***P* value**	**n**
44.9 %	55.1 %	1.44	0.23	136

Supplemental Materials

767 The following supplemental materials are available.
768
769 **Supplemental Figure 1.** Expression of candidate pollen *EXO70* genes during pollen
770 development in Arabidopsis.
771
772 **Supplemental Figure 2.** *EXO70C1* and *EXO70C2* expression in Arabidopsis roots.
773
774 **Supplemental Figure 3.** Positions of insertions in *exo70* mutant lines and semi-quantitative
775 RT-PCR analysis of gene expression of the affected *EXO70* isoforms.
776
777 **Supplemental Figure 4.** Propidium iodide staining of protoplast-like structures emerging
778 from the *exo70C2* pollen tube apex.
779
780 **Supplemental Figure 5.** Pollen tube lengths of complemented *exo70C2* lines non-segregating
781 for the *pEXO70C2::EXO70C2:GFP* expression cassette.
782
783 **Supplemental Figure 6.** Localization of *pEXO70C2*::GFP:EXO70C2 is identical to
784 *pEXO70C2*::EXO70C2:GFP.
785
786 **Supplemental Movie 1.** Growth dynamics of *exo70C2* and WT pollen tubes stained with
787 calcofluor white.
788
789 **Supplemental Movie 2.** Growth dynamics of *exo70C2* and WT pollen tubes stained with
790 calcofluor white.
791
792 **Supplemental Movie 3.** Multiple *exo70C2* pollen tube bursts and recovery.
793
794 **Supplemental Table 1.** List of primers used in this study.
795
796 **Supplemental File 1.** Interactive model of genetic segregation.
797
798
799 **Acknowledgements**
800

Special thanks belong to Martin Potocký (IEB ASCR, Prague) for helpful discussions on this project, on data presentation, and for boxplot rendering. The authors also thank to Roman Pleskot (IEB ASCR, Prague) for the sequence identity calculation, and Tsuyoshi Nakagawa for kindly providing pGWB vectors (Research Institute of Molecular Genetics, Shimane University). The T-DNA GABI lines analyzed here were generated in the context of the GABI-Kat program and provided by B. Weisshaar (MPI for Plant Breeding Research, Cologne).

Figure Legends

Figure 1. Expression of exocyst genes in Arabidopsis pollen.

A) Mean expression values in linear scale based on the ATH1 (Affymetrix) microarray data in Genevestigator. NA = not available on the ATH1 DNA chip.
B) Quantification of mRNA based on RNA-Seq data on mature pollen (Loraine et al., 2013).
C) Number of peptides detected in the proteome of mature pollen using mass spectroscopy (LC-MS/MS) (Grobei et al., 2009).

Figure 2. Pollen tube lengths of *exo70C2* mutants.

Distribution of pollen tube lengths in samples of *in vitro* germinated pollen from WT (A), *exo70C2* heterozygotes (B), and *exo70C2* homozygotes (C). Two independent lines of the same genotype are displayed in each graph; HT – heterozygous; HM – homozygous. At least 120 pollen tubes were measured for each line.
D) Box plots comparing the data from A–C.

Figure 3. Morphology of *exo70C2* pollen tubes germinated *in vitro*.

A–C) Germinated pollen of a WT plant (A), an *exo70C2* heterozygous plant (B), and an *exo70C2* homozygous plant (C) in the *quartet-1* background. Putative WT or mutant pollen tubes are marked by white or black arrows, respectively; arrows of the same design correspond to the same tetrad. Scale bars = 100 μm.

D) Distribution of pollen tube lengths in samples above (A–C).

E) A typical WT pollen tube. Scale bar = 20 μm.

F–K) Mutant pollen tubes showing relatively normal morphology (F), branching (G, I), sharp bending (H), effusion of cytoplasm (G, I; marked by arrowheads), or production of protoplast-like structures emerging from tube tips (J, K; marked by asterisks). Scale bars = 20 μm.

L) Aniline blue staining of pollinated pistils of a wild type and *exo70C2* homozygote visualizing callose in pollen tubes. Scale bar = 200 μm.

Figure 4. Growth rate and cell wall characteristics of *exo70C2* and WT pollen tubes.

A) Growth rate of a typical WT and *exo70C2* pollen tube correlated with cell wall thickness (calcofluor white fluorescence) at the tube apex. Images for measurement were captured at intervals of 5 s.

B) The averaged maximal growth rate of *exo70C2* is significantly higher than that of WT (SD is displayed; * Student's t-test *P* value < 0.00001). Measurements were performed on 15 tubes per genotype at multiple timepoints every 90 s.

C) Calcofluor white fluorescence represented as an intensity color scale (purple to white) shows differential cell wall deposition at the tube apex during highly fluctuating growth rate of the *exo70C2* pollen tube compared to WT characterized by low oscillations.

D) Pollen tubes of WT and *exo70C2* germinated and stained on the same slide with ruthenium red diluted in distilled water to cause the extrusion of cytoplasm. Details of burst tips that were used for quantification are inserted.

E) Quantification of the ruthenium red staining in extruded cytoplasm as relative intensity in the red channel subtracted from the background. is displayed; * Student's t-test *P* value < 10^{-10}; SD n = 50 for each genotype.

F) Propidium iodide staining of growing pollen tubes. Maximum intensity projection over a confocal Z-stack. Asterisks mark sites of collapses; arrowheads point to sites of stopped growth.

865 **Figure 5.** Pollen tube lengths of *exo70C2* lines complemented with
866 *pEXO70C2::*EXO70C2:GFP.
867
868 A) A representative microscopic image from the series used for pollen tube length analysis
869 above. Longer pollen tubes emitting *pEXO70C2::EXO70C2:GFP* fluorescence represent
870 complemented *exo70C2* mutant pollen tubes. GFP fluorescence mixed with bright field. Scale
871 bar = 100 µm.
872 B) Distribution of pollen tube lengths in samples of *in vitro* germinated pollen from
873 homozygous *exo70C2* mutants in which the introduced *pEXO70C2::EXO70C2:GFP* was in a
874 heterozygous state. Fluorescent and non-fluorescent pollen tubes were measured separately
875 within each sample. Two independent lines (1 and 2) were analyzed. Box plots inserted are
876 another presentation of the same data.
877
878
879 **Figure 6.** Localization of EXO70C1:GFP and EXO70C2:GFP expressed under their native
880 promoters in cells of *exo70C1* or *exo70C2* homozygotes, respectively.
881
882 A) EXO70C1:GFP and EXO70C2:GFP in mature pollen grains (the fluorescence intensity in
883 both samples not to scale). In addition, EXO70C1:GFP accumulates in the vegetative nucleus
884 (marked by arrow). Expression cassettes were segregating in the samples – non-fluorescent
885 pollen grains provide reference for the background fluorescence. Scale bars = 10 µm.
886 B) EXO70C1:GFP and EXO70C2:GFP in the cytoplasm of pollen tubes. Scale bars = 10 µm.
887 C) EXO70C1:GFP and EXO70C2:GFP in roots. The expression of EXO70C1 starts already
888 in the late meristem. Gray dotted lines mark root tips. Scale bars = 100 µm.
889 D) EXO70C1:GFP and EXO70C2:GFP are specifically expressed in trichoblast cells in roots
890 (maximum intensity projection of confocal Z-stacks). Scale bars = 20 µm.
891 E) Top views at 3D reconstructions calculated from the Z-stacks in (D).
892 F) While EXO70C1:GFP localizes to the cytoplasm and nucleus in elongated trichoblast cells,
893 EXO70C2:GFP is localized exclusively in the cytoplasm. Nuclei marked by arrows. Cell
894 walls stained with propidium iodide (in magenta). Scale bars = 10 µm.
895 G) Cytoplasmic localization of EXO70C1:GFP and EXO70C1:GFP in growing root hairs.
896 Cell walls stained with propidium iodide (in magenta). Scale bars = 10 µm.

H) The onset of EXO70C1:GFP expression in the root meristem. EXO70C1:GFP accumulates in the perinuclear region and/or nucleolus at certain stages. Cell walls stained with propidium iodide (in magenta). Scale bar = 10 µm.

Figure 7. Localization of EXO70C1 and EXO70C2 in comparison to core exocyst subunits in Arabidopsis pollen tubes and root hairs.

A) GFP:SEC8 and SEC10a:GFP exhibit a plasma-membrane association in the apex of growing pollen tubes in contrast to EXO70C1:GFP and EXO70C2:GFP that show cytoplasmic localization. Averaged time series (5 sequential images taken at 4s intervals) and one representative single image out of the series are displayed. Scale bar = 10 µm.
B) Co-localization of EXO70C2:GFP (green) and RFP:EXO70A1 (magenta) in growing root hairs shows no overlap. Scale bar = 10 µm.

Figure 8. EXO70C2 and EXO70A2 interactions in the yeast two-hybrid assay.
A) Pair-wise interactions with core exocyst subunits: EXO70A1–SEC3a and EXO70A1–EXO84b-N interactions described in Hála et al. (2008) were used as positive controls. Empty vectors pGADT7 (AD) and pGBKT7 (BD) were used as negative controls. BD-SEC3a and BD-SEC10b were omitted in this assay since they show high auto-activation capacity (Hála et al., 2008).
B) AD-EXO70C2 interacts with BD-ROH1, a putative negative regulator of secretion, similar to AD-EXO70C1 published in Kulich et al. (2010).

Parsed Citations

Alonso JM, Stepanova AN, Leisse TJ, Kim CJ, Chen H, Shinn P, Stevenson DK, Zimmerman J, Barajas P, Cheuk R, Gadrinab C, Heller C, Jeske A, Koesema E, Meyers CC, Parker H, Prednis L, Ansari Y, Choy N, Deen H, Geralt M, Hazari N, Hom E, Karnes M, Mulholland C, Ndubaku R, Schmidt I, Guzman P, Aguilar-Henonin L, Schmid M, Weigel D, Carter DE, Marchand T, Risseeuw E, Brogden D, Zeko A, Crosby WL, Berry CC, Ecker JR (2003) Genome-wide insertional mutagenesis of Arabidopsis thaliana. Science 301: 653-657

Pubmed: Author and Title
CrossRef: Author and Title
Google Scholar: Author Only Title Only Author and Title

Bashline L, Lei L, Li S, Gu Y (2014) Cell wall, cytoskeleton, and cell expansion in higher plants. Mol Plant 4: 586-600

Pubmed: Author and Title
CrossRef: Author and Title
Google Scholar: Author Only Title Only Author and Title

Bloch D, Pleskot R, Pejchar P, Potocký M, Trpkošová P, Cwiklik L, Vukašinovic N, Sternberg H, Yalovsky S, Žárský V (2016) Exocyst SEC3 and Phosphoinositides Define Sites of Exocytosis in Pollen Tube Initiation and Growth. Plant Physiol 172: 980-1002

Pubmed: Author and Title
CrossRef: Author and Title
Google Scholar: Author Only Title Only Author and Title

Chebli Y, Kaneda M, Zerzour R, Geitmann A (2012) The cell wall of the Arabidopsis pollen tube-spatial distribution, recycling, and network formation of polysaccharides. Plant Physiol 160: 1940-1955

Pubmed: Author and Title
CrossRef: Author and Title
Google Scholar: Author Only Title Only Author and Title

Chebli Y, Kroeger J, Geitmann A (2013) Transport logistics in pollen tubes. Mol Plant 6: 1037-1052.

Pubmed: Author and Title
CrossRef: Author and Title
Google Scholar: Author Only Title Only Author and Title

Cheung AY, Wu HM (2008) Structural and signaling networks for the polar cell growth machinery in pollen tubes. Annu Rev Plant Biol 59: 547-72

Pubmed: Author and Title
CrossRef: Author and Title
Google Scholar: Author Only Title Only Author and Title

Clough SJ, Bent AF (1998) Floral dip: a simplified method for Agrobacterium-mediated transformation of Arabidopsis thaliana. Plant J 16: 735-743

Pubmed: Author and Title
CrossRef: Author and Title
Google Scholar: Author Only Title Only Author and Title

Cole RA, Fowler JE (2006) Polarized growth: maintaining focus on the tip. Curr Opin Plant Biol 9: 579-588

Pubmed: Author and Title
CrossRef: Author and Title
Google Scholar: Author Only Title Only Author and Title

Cole RA, McInally SA, Fowler JE (2014) Developmentally distinct activities of the exocyst enable rapid cell elongation and determine meristem size during primary root growth in Arabidopsis. BMC Plant Biol 14: 386

Pubmed: Author and Title
CrossRef: Author and Title
Google Scholar: Author Only Title Only Author and Title

Cole RA, Synek L, Žárský V, Fowler JE (2005) SEC8, a subunit of the putative Arabidopsis exocyst complex, facilitates pollen germination and competitive pollen tube growth. Plant Physiol 138: 2005-2018

Pubmed: Author and Title
CrossRef: Author and Title
Google Scholar: Author Only Title Only Author and Title

Cvrcková F, Bezvoda R, Žárský V (2010) Computational identification of root hair-specific genes in Arabidopsis. Plant Signal Behav 5: 1407-1418

Pubmed: Author and Title
CrossRef: Author and Title
Google Scholar: Author Only Title Only Author and Title

Cvrcková F, Eliáš M, Hála M, Obermeyer G, Žárský V (2001) Small GTPases and conserved signalling pathways in plant cell morphogenesis: From exocytosis to Exocyst. In Cell Biology of Plant and Fungal Tip Growth (Geitmann, A and Cresti, M, eds), Amsterdam: IOS Press, 105-122

Pubmed: Author and Title
CrossRef: Author and Title
Google Scholar: Author Only Title Only Author and Title

Cvrcková F, Grunt M, Bezvoda R, Hála M, Kulich I, Rawat A, Žárský, V (2012) Evolution of the land plant exocyst complexes. Front Plant Sci 3: 159

Pubmed: Author and Title
CrossRef: Author and Title

Google Scholar: Author Only Title Only Author and Title

Dellago H, Löscher M, Ajuh P, Ryder U, Kaisermayer C, Grillari-Voglauer R, Fortschegger K, Gross S, Gstraunthaler A, Borth N, Eisenhaber F, Lamond AI, Grillari J (2011) Exo70, a subunit of the exocyst complex, interacts with SNEV (hPrp19/hPso4) and is involved in pre-mRNA splicing. Biochem J 438: 81-91
Pubmed: Author and Title
CrossRef: Author and Title
Google Scholar: Author Only Title Only Author and Title

Drdová EJ, Synek L, Pecenková T, Hála M, Kulich I, Fowler J E, Murphy A, Žárský V (2013) The exocyst complex contributes to PIN auxin efflux carrier recycling and polar auxin transport in Arabidopsis. Plant J 73: 709-719
Pubmed: Author and Title
CrossRef: Author and Title
Google Scholar: Author Only Title Only Author and Title

Edwards K, Johnstone C, Thompson C (1991) A simple and rapid method for the preparation of plant genomic DNA for PCR analysis. Nucl Acid Res 19: 1349
Pubmed: Author and Title
CrossRef: Author and Title
Google Scholar: Author Only Title Only Author and Title

Eliáš M, Drdová E, Ziak D, Bavlnka B, Hála M, Cvrcková F, Soukupová H, Žárský V (2003) The exocyst complex in plants. Cell Biol Int 27: 199-201
Pubmed: Author and Title
CrossRef: Author and Title
Google Scholar: Author Only Title Only Author and Title

Fendrych M, Synek L, Pecenková T, Drdová EJ, Sekereš J, De Rycke R, Nowack MK, Žárský V (2013) Visualization of the exocyst complex dynamics at the plasma membrane of Arabidopsis thaliana. Mol Biol Cell 24: 510-520
Pubmed: Author and Title
CrossRef: Author and Title
Google Scholar: Author Only Title Only Author and Title

Fendrych M, Synek L, Pecenková T, Toupalová H, Cole R, Drdová E, Nebesárová J, Šedinová M, Hála M, Fowler JE, Žárský V (2010) The Arabidopsis exocyst complex is involved in cytokinesis and cell plate maturation. Plant Cell 22: 3053-3065
Pubmed: Author and Title
CrossRef: Author and Title
Google Scholar: Author Only Title Only Author and Title

Fu Y (2015) The cytoskeleton in the pollen tube. Curr Opin Plant Biol 28: 111-119
Pubmed: Author and Title
CrossRef: Author and Title
Google Scholar: Author Only Title Only Author and Title

Grobei MA, Qeli E, Brunner E, Rehrauer H, Zhang R, Roschitzki B, Basler K, Ahrens CH, Grossniklaus U (2009) Deterministic protein inference for shotgun proteomics data provides new insights into Arabidopsis pollen development and function. Genome Res 19: 1786-800
Pubmed: Author and Title
CrossRef: Author and Title
Google Scholar: Author Only Title Only Author and Title

Guo W, Grant A, Novick P (1999) Exo84p is an exocyst protein essential for secretion. J Biol Chem 33: 23558-23564
Pubmed: Author and Title
CrossRef: Author and Title
Google Scholar: Author Only Title Only Author and Title

Hála M, Cole R, Synek L, Drdová E, Pecenková T, Nordheim A, Lamkemeyer T, Madlung T, Hochholdinger F, Fowler JE, Žárský V (2008) An exocyst complex functions in plant cell growth in Arabidopsis and tobacco. Plant Cell 20: 1330-1345
Pubmed: Author and Title
CrossRef: Author and Title
Google Scholar: Author Only Title Only Author and Title

Heider MR, Munson M (2012) Exorcising the Exocyst Complex. Traffic 13: 898-907
Pubmed: Author and Title
CrossRef: Author and Title
Google Scholar: Author Only Title Only Author and Title

Hepler PK, Rounds CM, Winship LJ (2013) Control of cell wall extensibility during pollen tube growth. Mol Plant 6: 998-1017
Pubmed: Author and Title
CrossRef: Author and Title
Google Scholar: Author Only Title Only Author and Title

Hepler PK, Winship LJ (2015) The pollen tube clear zone: clues to the mechanism of polarized growth. J Integr Plant Biol 57: 79-92
Pubmed: Author and Title
CrossRef: Author and Title
Google Scholar: Author Only Title Only Author and Title

Hong D, Jeon BW, Kim SY, Hwang JU, Lee Y (2016) The ROP2-RIC7 pathway negatively regulates light-induced stomatal opening by inhibiting exocyst subunit EXO70B1 in Arabidopsis. New Phytol 209: 624-35
Pubmed: Author and Title
CrossRef: Author and Title

Google Scholar: Author Only Title Only Author and Title

Ito T, Motohashi R, Kuromori T, Mizukado S, Sakurai T, Kanahara H, Seki M, Shinozaki K (2002) A new resource of locally transposed Dissociation elements for screening gene-knockout lines in silico on the Arabidopsis genome. Plant Physiol 129: 1695-1699
Pubmed: Author and Title
CrossRef: Author and Title
Google Scholar: Author Only Title Only Author and Title

Johnson-Brousseau SA, McCormick S (2004) A compendium of methods useful for characterizing Arabidopsis pollen mutants and gametophytically-expressed genes. Plant J 39:761-775
Pubmed: Author and Title
CrossRef: Author and Title
Google Scholar: Author Only Title Only Author and Title

Karimi M, Inzé D, Depicker A (2002) GATEWAY™ vectors for Agrobacterium-mediated plant transformation. Trends in Plant Sci 7: 193-195
Pubmed: Author and Title
CrossRef: Author and Title
Google Scholar: Author Only Title Only Author and Title

Kitashiba H, Liu P, Nishio T, Nasrallah JB, Nasrallah ME (2011) Functional test of Brassica self-incompatibility modifiers in Arabidopsis thaliana. Proc Natl Acad Sci U S A 108: 18173-8
Pubmed: Author and Title
CrossRef: Author and Title
Google Scholar: Author Only Title Only Author and Title

Kleinboelting N, Huep G, Kloetgen A, Viehoever P, Weisshaar B (2012) GABI-Kat SimpleSearch: new features of the Arabidopsis thaliana T-DNA mutant database. Nucleic Acids Res 40: D1211-1215.
Pubmed: Author and Title
CrossRef: Author and Title
Google Scholar: Author Only Title Only Author and Title

Kulich I, Cole R, Drdová E, Cvrcková F, Soukup A, Fowler JE, Žárský V (2010) Arabidopsis exocyst subunits SEC8 and EXO70A1 and exocyst interactor ROH1 are involved in the localized deposition of seed coat pectin. New Phytol 188: 615-625
Pubmed: Author and Title
CrossRef: Author and Title
Google Scholar: Author Only Title Only Author and Title

Kulich I, Pecenková T, Sekereš J, Smetana O, Fendrych M, Foissner I, Höftberger M, Žárský V (2013) Arabidopsis exocyst subcomplex containing subunit EXO70B1 is involved in autophagy-related transport to the vacuole. Traffic 14: 1155-1165
Pubmed: Author and Title
CrossRef: Author and Title
Google Scholar: Author Only Title Only Author and Title

Kulich I, Vojtíková Z, Glanc M, Ortmannová J, Rasmann S, Žárský V (2015) Cell Wall Maturation of Arabidopsis Trichomes Is Dependent on Exocyst Subunit EXO70H4 and Involves Callose Deposition. Plant physiol 168: 120-131
Pubmed: Author and Title
CrossRef: Author and Title
Google Scholar: Author Only Title Only Author and Title

Kuromori T, Hirayama T, Kiyosue Y, Takabe H, Mizukado S, Sakurai T, Akiyama K, Kamiya A, Ito T, Shinozaki K (2004) A collection of 11800 single-copy Ds transposon insertion lines in Arabidopsis. Plant J 37: 897-905
Pubmed: Author and Title
CrossRef: Author and Title
Google Scholar: Author Only Title Only Author and Title

Lai KS (2016) Analysis of EXO70C2 expression revealed its specific association with late stages of pollen development. Plant Cell Tiss Organ Cult 124: 209-215
Pubmed: Author and Title
CrossRef: Author and Title
Google Scholar: Author Only Title Only Author and Title

Lassig R, Gutermuth T, Bey TD, Konrad KR, Romeis T (2014) Pollen tube NAD(P)H oxidases act as a speed control to dampen growth rate oscillations during polarized cell growth. Plant J 78: 94-106
Pubmed: Author and Title
CrossRef: Author and Title
Google Scholar: Author Only Title Only Author and Title

Lavy M, Bloch D, Hazak O, Gutman I, Poraty L, Sorek N, Sternberg H, Yalovsky S (2007) A Novel ROP/RAC effector links cell polarity, root-meristem maintenance, and vesicle trafficking. Curr Biol 17: 947-952
Pubmed: Author and Title
CrossRef: Author and Title
Google Scholar: Author Only Title Only Author and Title

Li S, Chen M, Yu D, Ren S, Sun S, Liu L, Ketelaar T, Emons AMC, Liu CM (2013) EXO70A1-mediated vesicle trafficking is critical for tracheary element development in Arabidopsis. Plant Cell 25: 1774-1786
Pubmed: Author and Title
CrossRef: Author and Title
Google Scholar: Author Only Title Only Author and Title

Li S, van Os GM, Ren S, Yu D, Ketelaar T, Emons AMC, Liu CM (2010) Expression and functional analyses of EXO70 genes in Arabidopsis implicate their roles in regulating cell type-specific exocytosis. Plant Physiol 154: 1819-1830
Pubmed: Author and Title
CrossRef: Author and Title
Google Scholar: Author Only Title Only Author and Title

Liu J, Guo W (2012) The exocyst complex in exocytosis and cell migration. Protoplasma 249: 587-597
Pubmed: Author and Title
CrossRef: Author and Title
Google Scholar: Author Only Title Only Author and Title

Loraine AE, McCormick S, Estrada A, Patel K, Qin P (2013) RNA-seq of Arabidopsis pollen uncovers novel transcription and alternative splicing. Plant Physiol 162: 1092-1109
Pubmed: Author and Title
CrossRef: Author and Title
Google Scholar: Author Only Title Only Author and Title

MacAlister CA, OrtizRamírez C, Becker JD, Feijó JA, Lippman ZB (2016) Hydroxyproline Oarabinosyltransferase mutants oppositely alter tip growth in Arabidopsis thaliana and Physcomitrella patens. Plant J 85: 193-208
Pubmed: Author and Title
CrossRef: Author and Title
Google Scholar: Author Only Title Only Author and Title

Mayank P, Grossman J, Wuest S, Boisson-Dernier A, Roschitzki B, Nanni P, Nühse T, Grossniklaus U (2012) Characterization of the phosphoproteome of mature Arabidopsis pollen. Plant J 72: 89-101
Pubmed: Author and Title
CrossRef: Author and Title
Google Scholar: Author Only Title Only Author and Title

McKenna ST, Kunkel JG, Bosch M, Rounds CM, Vidali L, Winship LJ, Hepler PK (2009) Exocytosis precedes and predicts the increase in growth in oscillating pollen tubes. Plant Cell 21: 3026-3040.
Pubmed: Author and Title
CrossRef: Author and Title
Google Scholar: Author Only Title Only Author and Title

Mori T, Kuroiwa H, Higashiyama T, Kuroiwa T (2006) Generative Cell Specific 1 is essential for angiosperm fertilization. Nat Cell Biol 8: 64-71
Pubmed: Author and Title
CrossRef: Author and Title
Google Scholar: Author Only Title Only Author and Title

Moscatelli A, Idilli AI (2009) Pollen tube growth: a delicate equilibrium between secretory and endocytic pathways. J Integr Plant Biol 51: 727-39
Pubmed: Author and Title
CrossRef: Author and Title
Google Scholar: Author Only Title Only Author and Title

Nakagawa T, Kurose T, Hino T, Tanaka K, Kawamukai M, Niwa Y, Toyooka K, Matsuoka K, Jinbo T, Kimura T (2007) Development of series of gateway binary vectors, pGWBs, for realizing efficient construction of fusion genes for plant transformation. J Biosci Bioeng 104: 34-41
Pubmed: Author and Title
CrossRef: Author and Title
Google Scholar: Author Only Title Only Author and Title

Pecenková T, Hála M, Kulich I, Kocourková D, Drdová E, Fendrych M, Toupalová H, Žárský V (2011) The role for the exocyst complex subunits Exo70B2 and Exo70H1 in the plant-pathogen interaction. J Exp Bot 62: 2107-2116
Pubmed: Author and Title
CrossRef: Author and Title
Google Scholar: Author Only Title Only Author and Title

Pfeffer SR (2013) Rab GTPase regulation of membrane identity. Curr Opin Cell Biol 25: 414-419.
Pubmed: Author and Title
CrossRef: Author and Title
Google Scholar: Author Only Title Only Author and Title

Picton JM, Steer MW (1983). Membrane recycling and the control of secretory activity in pollen tubes. J Cell Sci 63: 303-310
Pubmed: Author and Title
CrossRef: Author and Title
Google Scholar: Author Only Title Only Author and Title

Preuss D, Rhee SY, Davis RW (1994) Tetrad analysis possible in Arabidopsis with mutation of the QUARTET (QRT) genes. Science 264: 1458-1460
Pubmed: Author and Title
CrossRef: Author and Title
Google Scholar: Author Only Title Only Author and Title

Rounds CM, Lubeck E, Hepler PK, Winship LJ (2011) Propidium iodide competes with Ca2+ to label pectin in pollen tubes and Arabidopsis root hairs. Plant Physiol 157: 175-187
Pubmed: Author and Title
CrossRef: Author and Title
Google Scholar: Author Only Title Only Author and Title

Rutley N, Twell D (2015) A decade of pollen transcriptomics. Plant Reprod 28: 73-89
Pubmed: Author and Title
CrossRef: Author and Title
Google Scholar: Author Only Title Only Author and Title

Rybak K, Steiner A, Synek L, Klaeger S, Kulich I, Facher E, Wanner G, Kuster B, Žárský V, Persson S, Assaad FF (2014) Plant cytokinesis is orchestrated by the sequential action of the TRAPPII and Exocyst tethering complexes. Dev Cell 29: 607-620
Pubmed: Author and Title
CrossRef: Author and Title
Google Scholar: Author Only Title Only Author and Title

Safavian D, Zayed Y, Indriolo E, Chapman L, Ahmed A, Goring DR (2015) RNA Silencing of Exocyst Genes in the Stigma Impairs the Acceptance of Compatible Pollen in Arabidopsis. Plant Physiol 169: 2526-2538
Pubmed: Author and Title
CrossRef: Author and Title
Google Scholar: Author Only Title Only Author and Title

Samuel MA, Chong YT, Haasen KE, Aldea-Brydges MG, Stone SL, Goring DR (2009) Cellular pathways regulating responses to compatible and self-incompatible pollen in Brassica and Arabidopsis stigmas intersect at Exo70A1, a putative component of the exocyst complex. Plant Cell 21: 2655-71
Pubmed: Author and Title
CrossRef: Author and Title
Google Scholar: Author Only Title Only Author and Title

Sanati Nezhad A, Packirisamy M, Geitmann A (2014) Dynamic, high precision targeting of growth modulating agents is able to trigger pollen tube growth reorientation. Plant J 80: 185-195
Pubmed: Author and Title
CrossRef: Author and Title
Google Scholar: Author Only Title Only Author and Title

Schindelin J, Arganda-Carreras I, Frise E, Kaynig V, Longair M, Pietzsch T, Preibisch S, Rueden C, Saalfeld S, Schmid B, Tinevez JY, White DJ, Hartenstein V, Eliceiri K, Tomancak P, Cardona A (2012) Fiji: an open-source platform for biological-image analysis. Nat Methods 9: 676-682
Pubmed: Author and Title
CrossRef: Author and Title
Google Scholar: Author Only Title Only Author and Title

Schwab R, Ossowski S, Riester M, Warthmann N, Weigel D (2006) Highly specific gene silencing by artificial microRNAs in Arabidopsis. Plant Cell 18: 1121-1133
Pubmed: Author and Title
CrossRef: Author and Title
Google Scholar: Author Only Title Only Author and Title

Sekereš J, Pejchar P, Šantrucek J, Vukašinovic N, Žárský V, Potocký M (2017) Analysis of exocyst subunit EXO70 family reveals distinct membrane domains in tobacco pollen tubes. Plant Physiol 173: 1659-1675
Pubmed: Author and Title
CrossRef: Author and Title
Google Scholar: Author Only Title Only Author and Title

Stegmann M, Anderson RG, Ichimura K, Pecenková T, Reuter P, Žárský V, McDowell JM, Shirasu K, Trujillo M (2012) The ubiquitin ligase PUB22 targets a subunit of the exocyst complex required for PAMP-triggered responses in Arabidopsis. Plant Cell, 24: 4703-4716
Pubmed: Author and Title
CrossRef: Author and Title
Google Scholar: Author Only Title Only Author and Title

Synek L, Schlager N, Eliáš M, Quentin M, Hauser MT, Žárský V (2006) AtEXO70A1, a member of a family of putative exocyst subunits specifically expanded in land plants, is important for polar growth and plant development. Plant J 48: 54-72
Pubmed: Author and Title
CrossRef: Author and Title
Google Scholar: Author Only Title Only Author and Title

TerBush DR, Maurice T, Roth D, Novick P (1996) The Exocyst is a multiprotein complex required for exocytosis in Saccharomyces cerevisiae. EMBO J 15: 6483-6494
Pubmed: Author and Title
CrossRef: Author and Title
Google Scholar: Author Only Title Only Author and Title

TerBush DR, Novick P (1995) Sec6, Sec8, and Sec15 are components of a multisubunit complex which localizes to small bud tips in Saccharomyces cerevisiae. J Cell Biol 130: 299-312
Pubmed: Author and Title
CrossRef: Author and Title
Google Scholar: Author Only Title Only Author and Title

Tu B, Hu L, Chen W, Li T, Hu B, Zheng L, Lv Z, You S, Wang Y, Ma B, Chen X, Qin P, Li S (2015) Disruption of OsEXO70A1 Causes Irregular Vascular Bundles and Perturbs Mineral Nutrient Assimilation in Rice. Sci Rep 5: 18609
Pubmed: Author and Title
CrossRef: Author and Title
Google Scholar: Author Only Title Only Author and Title

Vega IE, Hsu SC (2001) The exocyst complex associates with microtubules to mediate vesicle targeting and neurite outgrowth. J Neurosci 21: 3839-3848
Pubmed: Author and Title
CrossRef: Author and Title
Google Scholar: Author Only Title Only Author and Title

Vukašinovic N, Cvrcková F, Eliáš M, Cole R, Fowler JE, Žárský V, Synek L (2014) Dissecting a Hidden Gene Duplication: The Arabidopsis thaliana SEC10 Locus. PloS one 9: e94077
Pubmed: Author and Title
CrossRef: Author and Title
Google Scholar: Author Only Title Only Author and Title

Vukašinovic N, Oda Y, Pejchar P, Synek L, Pecenková T, Rawat A, Sekereš J, Potocký M, Žárský V (2016) Microtubule-Dependent Targeting of the Exocyst Complex is Necessary for the Xylem Development in Arabidopsis. New Phytol, doi: 10.1111/nph.14267
Pubmed: Author and Title
CrossRef: Author and Title
Google Scholar: Author Only Title Only Author and Title

Vukašinovic N, Žárský V (2016) Tethering Complexes in the Arabidopsis Endomembrane System. Front Cell Dev Biol 4: 46
Pubmed: Author and Title
CrossRef: Author and Title
Google Scholar: Author Only Title Only Author and Title

Wang S, Liu Y, Adamson CL, Valdez G, Guo W, Hsu SC (2004) The mammalian exocyst, a complex required for exocytosis, inhibits tubulin polymerization. J Biol Chem 279: 35958-66
Pubmed: Author and Title
CrossRef: Author and Title
Google Scholar: Author Only Title Only Author and Title

Wei LQ, Xu WY, Deng ZY, Su Z, Xue Y, Wang T (2010) Genome-scale analysis and comparison of gene expression profiles in developing and germinated pollen in Oryza sativa. BMC Genomics 11: 338
Pubmed: Author and Title
CrossRef: Author and Title
Google Scholar: Author Only Title Only Author and Title

Wen-Chi Hou WC, Chang WH, Jiang CM (1999) Qualitative distinction of carboxyl group distributions in pectins with ruthenium red. Bot Bull Acad Sin 40: 115-119
Pubmed: Author and Title
CrossRef: Author and Title
Google Scholar: Author Only Title Only Author and Title

Winter D, Vinegar B, Nahal H, Ammar R, Wilson G V, Provart NJ (2007) An "Electronic Fluorescent Pictograph" browser for exploring and analyzing large-scale biological data sets. PloS one 2: e718
Pubmed: Author and Title
CrossRef: Author and Title
Google Scholar: Author Only Title Only Author and Title

Wu H, Rossi G, Brennwald P (2008) The ghost in the machine: small GTPases as spatial regulators of exocytosis. Trends Cell Biol 18: 397-404
Pubmed: Author and Title
CrossRef: Author and Title
Google Scholar: Author Only Title Only Author and Title

Žárský V, Cvrcková F, Potocký M, Hála M (2009) Exocytosis and cell polarity in plants-exocyst and recycling domains. New Phytol 183: 255-272
Pubmed: Author and Title
CrossRef: Author and Title
Google Scholar: Author Only Title Only Author and Title

Žárský V, Kulich I, Fendrych M, Pecenková T (2013) Exocyst complexes multiple functions in plant cells secretory pathways. Curr Opin Plant Biol 16: 726-733
Pubmed: Author and Title
CrossRef: Author and Title
Google Scholar: Author Only Title Only Author and Title

Žárský V, Potocký M (2010) Recycling domains in plant cell morphogenesis: small GTPase effectors, plasma membrane signalling and the exocyst. Biochem Soc Trans 38: 723-728
Pubmed: Author and Title
CrossRef: Author and Title
Google Scholar: Author Only Title Only Author and Title

Zhang C, Brown MQ, van de Ven W, Zhang ZM, Wu B, Young MC, Synek L, Borchardt D, Harrison R, Pan S, Luo N, Huang YM, Ghang YJ, Ung N, Li R, Isley J, Morikis D, Song J, Guo W, Hooley RJ, Chang CE, Yang Z, Zarsky V, Muday GK, Hicks GR, Raikhel NV (2016) Endosidin2 targets conserved exocyst complex subunit EXO70 to inhibit exocytosis. Proc Natl Acad Sci USA 113: E41-50
Pubmed: Author and Title
CrossRef: Author and Title
Google Scholar: Author Only Title Only Author and Title

Zhang X, Pumplin N, Ivanov S, Harrison MJ (2015) EXO70I is required for development of a sub-domain of the periarbuscular membrane during arbuscular mycorrhizal symbiosis. Curr Biol 25: 2189-2195

Pubmed: Author and Title
CrossRef: Author and Title
Google Scholar: Author Only Title Only Author and Title

Zhao Y, Liu J, Yang C, Capraro BR, Baumgart T, Bradley RP, Ramakrishnan N, Xu X, Radhakrishnan R, Svitkina T, Guo W (2013) Exo70 generates membrane curvature for morphogenesis and cell migration. Dev Cell 26: 266-278.
Pubmed: Author and Title
CrossRef: Author and Title
Google Scholar: Author Only Title Only Author and Title

Zimmermann P, Hirsch-Hoffmann M, Hennig L, Gruissem W (2004) GENEVESTIGATOR. Arabidopsis microarray database and analysis toolbox. Plant Physiol 136: 2621-2632
Pubmed: Author and Title
CrossRef: Author and Title
Google Scholar: Author Only Title Only Author and Title

Zonia L, Munnik T (2008) Vesicle trafficking dynamics and visualization of zones of exocytosis and endocytosis in tobacco pollen tubes. J Exp Bot 59: 861-73
Pubmed: Author and Title
CrossRef: Author and Title
Google Scholar: Author Only Title Only Author and Title

Zonia L, Munnik T (2009) Uncovering hidden treasures in pollen tube growth mechanics. Trends Plant Sci 14: 318-327
Pubmed: Author and Title
CrossRef: Author and Title
Google Scholar: Author Only Title Only Author and Title

Zuo X, Zhang J, Zhang Y, Hsu SC, Zhou D, Guo W (2006) Exo70 interacts with the Arp2/3 complex and regulates cell migration. Nat Cell Biol 8: 1383-1388
Pubmed: Author and Title
CrossRef: Author and Title
Google Scholar: Author Only Title Only Author and Title